Division of Pharmaceutical Technology
Faculty of Pharmacy
University of Helsinki
Helsinki

Characterisation and processing of amorphous binary mixtures with low glass transition temperature

Pekka Hoppu

ACADEMIC DISSERTATION

To be presented, with the permission of the Faculty of Pharmacy of the University of Helsinki, for public examination in lecture hall 3 at Building of Forest Sciences (Latokartanonkaari 7), on 19 September 2008, at 12 noon.

Helsinki 2008

Supervisors: Professor Anne Juppo
Division of Pharmaceutical Technology
Industrial Pharmacy
Faculty of Pharmacy
University of Helsinki
Finland

Associate Professor Staffan Schantz
AstraZeneca R&D
Mölndal
Sweden

Reviewers: Doctor James Patterson
Pharmaceutical Development
GlaxoSmithKline
Essex
United Kingdom

Professor Yrjö H. Roos
Department of Food and Nutritional Sciences
University College Cork
Cork
Ireland

Opponent: Professor Guy Van den Mooter
Laboratory of Pharmacotechnology and Biopharmacy
University of Leuven
Belgium

ISBN 978-952-10-4919-4 (paperback)
ISBN 978-952-10-4920-0 (PDF, http://ethesis.helsinki.fi)
ISSN 1795-7079

Helsinki University Printing House
Helsinki 2008
Finland

Abstract

Hoppu, P., 2008. **Characterisation and processing of amorphous binary mixtures with low glass transition temperature.** Dissertationes bioscientiarum molecularium Universitatis Helsingiensis in Viikki, 35/2008, 64 pp., ISBN 978-952-10-4919-4 (paperpack), ISBN 978-952-10-4920-0 (pdf), ISSN 1795-7079.

The number of drug substances in formulation development in the pharmaceutical industry is increasing. Some of these are amorphous drugs and have glass transition below ambient temperature, and thus they are usually difficult to formulate and handle. One reason for this is the reduced viscosity, related to the stickiness of the drug, that makes them complicated to handle in unit operations. Thus, the aim in this thesis was to develop a new processing method for a sticky amorphous model material. Furthermore, model materials were characterised before and after formulation, using several characterisation methods, to understand more precisely the prerequisites for physical stability of amorphous state against crystallisation.

The model materials used were monoclinic paracetamol and citric acid anhydrate. Amorphous materials were prepared by melt quenching or by ethanol evaporation methods. The melt blends were found to have slightly higher viscosity than the ethanol evaporated materials. However, melt produced materials crystallised more easily upon consecutive shearing than ethanol evaporated materials. The only material that did not crystallise during shearing was a 50/50 (w/w, %) blend regardless of the preparation method and it was physically stable at least two years in dry conditions. Shearing at varying temperatures was established to measure the physical stability of amorphous materials in processing and storage conditions.

The actual physical stability of the blends was better than the pure amorphous materials at ambient temperature. Molecular mobility was not related to the physical stability of the amorphous blends, observed as crystallisation. Molecular mobility of the 50/50 blend derived from a spectral linewidth as a function of temperature using solid state NMR correlated better with the molecular mobility derived from a rheometer than that of differential scanning calorimetry data. Based on the results obtained, the effect of molecular interactions, thermodynamic driving force and miscibility of the blends are discussed as the key factors to stabilise the blends.

The stickiness was found to be affected glass transition and viscosity. Ultrasound extrusion and cutting were successfully tested to increase the processability of sticky material. Furthermore, it was found to be possible to process the physically stable 50/50 blend in a supercooled liquid state instead of a glassy state. The method was not found to accelerate the crystallisation. This may open up new possibilities to process amorphous materials that are otherwise impossible to manufacture into solid dosage forms.

Acknowledgements

This study was carried out mainly at the Division of Pharmaceutical Technology, Faculty of Pharmacy at the University of Helsinki during the years 2004-2008.

The biggest thanks ever go to my supervisors Prof. Anne Juppo and Assoc Prof. Staffan Schantz who I especially thank for their never-ending guidance and understanding during these years.

I am grateful to my all co-supervisors Prof. Jukka Rantanen, and co-authors Assoc. Prof. Kirsi Jouppila, Assoc. Prof. Sami Hietala and Dr. Antti Grönroos, for their perseverance during this work.

I have been lucky to work with people of different personalities, with their various excellent skills, at the Division of Pharmaceutical Technology. At least I have grown up during the years that I have worked with these people.

In addition, several other professional places and people were involved in giving me an opportunity to carry out my experimental designs and to make this thesis achievable. These places were Department of Food Technology and Department of Polymer Chemistry at the University of Helsinki, AstraZeneca R&D in Mölndal in Sweden and the Technical Research Centre of Finland (VTT) in Jyväskylä, Finland. I gratefully acknowledge the people in these places all around the Nordic area giving me an opportunity to use their facilities and having discussions on interesting topics during the coffee and lunch breaks.

AstraZeneca R&D, Mölndal, Sweden is acknowledged for their financial support during all of these years. In addition, they gave me a reference group, which gave interesting views in my studies. In addition, discussions with them developed me as a researcher.

Docent Pirjo Luukkonen and Dr. Åsa Adolfsson are thanked for encouraging me during my M.Sc. studies in Mölndal Sweden (years 2002-2003). They gave me the motivation and good skills to continue my studies as a Ph.D. student. Without them, I would probably not have started my Ph.D. studies.

I especially want to thank my siblings, friends and wife who inspired me and gave me delight during all of these years. I am thankful to my parents Aarno and Tuula, who gave me a stimulating environment to grow up during my childhood and for their ceaseless encouragement and support throughout all my life.

Helsinki, September 2008

Pekka Hoppu

Table of contents

Abstract i
Acknowledgements ii
Table of contents iii
List of original publications v
Abbreviations vi
1. Introduction 1
2. Literature review 4
2.1 Processing methods to produce amorphous material 4
2.2 Properties of the amorphous state 6
2.2.1 Glass transition 6
2.2.2 Physical aging 9
2.3 Factors affecting physical stability of the amorphous state 10
2.3.1 Molecular interactions 11
2.3.2 Molecular mobility 12
2.3.3 Other factors affecting physical stability 14
2.4 Stickiness 15
2.4.1 Theories of adhesion 16
2.4.2 Factors causing stickiness 17
2.5 Processing amorphous or sticky material into a solid dosage form 19
2.5.1 Temperature and water content 19
2.5.2 Antiplasticizer 20
2.5.3 Drying methods 20
2.5.4 Dispersions 21
2.5.5 Melt extrusion 22
2.5.6 Loading into a porous structure 22
2.5.7 Microcapsules and microparticles 22
2.6 Ultrasound processing 23
2.6.1 Principles 23
2.6.2 Possibilities for ultrasound processing 24
2.6.3 Ultrasound cutting 25
3. Aims of the study 27
4. Experimental 28
4.1 Materials 28
4.2 Processing methods 28

4.2.1 Sample preparation of binary mixtures (I, II, III, IV, V) 28
4.2.2 Ultrasound extrusion and cutting (III) 30
4.3 Analytical methods 32
4.3.1 High-performance liquid chromatography (I, II, IV, V) 32
4.3.2 Water content analysis (I, II, IV, V) 32
4.3.3 Raman scattering (I) 32
4.3.4 Fourier transform infrared microscopy (I, II, IV) 32
4.3.5 Thermal analysis (I, II, IV, V) 33
4.3.6 X-ray powder diffraction (I, II, IV) 34
4.3.7 Resistance to deformation and stickiness (III) 34
4.3.8 Rheology (II) 35
4.3.9 Solid state nuclear magnetic resonance (V) 35
4.3.10 Optical and stereo microscopy (IV) 36
4.3.11 Aging study (I, II, IV) 37
4.3.12 Statistical methods (I, II, III, IV, V) 37
5. Results and discussion 38
5.1 Effect of composition and sample preparation method on amorphous binary mixtures 38
5.1.1 Glass transition temperature (I, II, IV, V) 38
5.1.2 Physical stability against crystallisation (I, II, IV, V) 40
5.1.3 Rheology (II, V) 43
5.2 Factors affecting physical stability of amorphous binary mixtures 45
5.2.1 Fragility parameters (II, V) 45
5.2.2 Molecular mobility (II, V) 45
5.2.3 Molecular interactions (I, II, V) 47
5.2.4 Homogeneity of materials (I, II, V) 48
5.2.5 Other prerequisites for physical stability (I, II, V) 49
5.3 Ultrasound-assisted processing 49
5.3.1 Extrusion (III) 50
5.3.2 Cutting (III) 51
5.3.3 Effect of ultrasound on physical stability of materials (IV) 52
6. Conclusions 53
7. References 54

List of original publications

This thesis is based on the following publications:

I **Hoppu, P.**, Jouppila, K., Rantanen, J., Schantz, S., Juppo., A.M. Characterisation of blends of paracetamol and citric acid. Journal of Pharmacy and Pharmacology 2007, 59, 373-381.

II **Hoppu, P.**, Hietala, S., Schantz, S., Juppo, A.M. Viscosity and molecular mobility of amorphous citric acid and paracetamol blends. European Journal of Pharmaceutics and Biopharmaceutics, In press.

III **Hoppu, P.**, Grönroos, A., Schantz, S., Juppo, A.M. New processing technique for viscous amorphous materials and characterization of their stickiness and deformability. Submitted.

IV **Hoppu, P.,** Virpioja, J., Schantz, S., Juppo, A.M. Characterization of ultrasound extruded and cut citric acid/paracetamol blends. Journal of Pharmaceutical Sciences, In press.

V Schantz, S., **Hoppu, P.**, Juppo, A.M. A solid-state NMR study of phase structure, molecular interactions and mobility in blends of citric acid and paracetamol. Journal of Pharmaceutical Sciences, In press.

The publications are referred to in the text by their roman numerals I-V.

Abbreviations

ϕ	relaxation function
ω	angular velocity
A	material parameter
AGV	Adam-Gibbs-Vogel
API	active pharmaceutical ingredient
c	crystalline
CAA	citric acid anhydrate
CAM	citric acid monohydrate
CP	cross polarisation
C_p	specific heat capacity
D	strength parameter
DC	proton decoupling
DSC	differential scanning calorimetry
EtOH	ethanol
FDA	U.S. Food and Drug Administration
g	glassy
G'	storage modulus
G''	loss modulus
HPLC	high performance liquid chromatography
KWW	Kohlrausch-Williams-Watts equation
l	liquid
MAS	magic angle spinning
MDSC	modulating DSC
PARA	paracetamol
25/75	binary mixture containing 25% (w/w) of PARA and 75% of CAA
50/50	binary mixture containing 50% (w/w) of PARA and 50% of CAA
75/25	binary mixture containing 75% (w/w) of PARA and 25% of CAA
R	gas constant
RAMP-CP	ramped amplitude cross polarisation
RH	relative humidity
s	solid
t	storage time
T	temperature
T_0	ideal glass transition temperature where relaxation times approach infinity
T_f	fictive temperature, temperature where a property of a non-equilibrium state (enthalpy/entropy) corresponds to that of an equilibrium state
T_f^0	initial fictive temperature
T_g	glass transition temperature
T_g^{mid}	T_g midpoint (extrapolated)
T_g^o	T_g onset (extrapolated)
T_k	Kauzmann temperature
VTF	Vogel-Tamman-Fulcher

XRPD	X-ray powder diffraction
β	mean relaxation time distribution constant (KWW)
γ	related to C_p ratio of the crystalline (c) and glassy (g) material at T_g
ΔC_p	change in specific heat capacity at T_g
ΔH	enthalpy relaxation
ΔH_{oo}	maximum enthalpy recovery
τ	molecular relaxation time
τ_0	pre-exponential factor (approx. similar to vibrational lifetimes 10^{-14}s)
τ^0	initial relaxation time of AGV
τ^{kww}	mean molecular relaxation time constant (KWW)
η	viscosity
η^*	complex viscosity

1. Introduction

An active pharmaceutical ingredient (API) may exist in different physical forms. The polymorphism of crystalline drugs is the main focus in solid-state pharmacy. In crystalline polymorphs, molecules can have different internal arrangements and conformations in the crystal lattice, and thus they have long-range molecular order. The most stable polymorphic form has the lowest possibility for conversion to other polymorphic forms during processing or storage and thus it is the one formulated into a drug product. Nowadays, metastable forms are also chosen for formulation in order to increase solubility, for instance, and thereby bioavailability of the drug.

Amorphous materials are non-equilibrium systems and many changes in the materials have time-dependent properties [1]. An amorphous solid has short-range molecular order but it does not have any long-range molecular order or packing as a crystalline form would. Typically, these regions of short-range order have size of only a few molecular layers [2]. Amorphous structures are observed widely in nature, where carbohydrate glasses play an important role in the anhydrous preservation of biological systems. An amorphous structure is common for polymeric materials, food ingredients, peptides and proteins that are naturally amorphous, most likely owing to their large molecular size or due to their processing.

In pharmaceutical materials, an amorphous state is common for excipients and it increases within drug molecules, especially within biopharmaceuticals that are also naturally amorphous or they are often formulated into an amorphous matrix to increase chemical stability [3]. Rational drug design and high throughput screening have changed the development of new drugs. Specific understanding of more complex receptor structure usually results in larger and more complex molecular structures for drugs that bind to these receptors. New drugs are modified to suit complex receptors, and this has increased problems in drug development, such as difficulties in crystallising drugs [4]. Modification increases size and complexity, producing molecules that are difficult to crystallise.

The amorphous solid state has a higher dissolution* rate (*NOTE: In this study, the term dissolution is also used for an amorphous material although the amorphous material mixes into liquid. The term dissolution is appropriate for crystalline material.), higher chemical reactivity and higher water vapour sorption than the crystalline state. This is due to increased free volume, molecular mobility and the enthalpy of the amorphous state [2]. These properties can have benefits. For example, rapid formation of solution is sometimes desirable to achieve a high efficacy and a rapid absorption rate that may increase the bioavailability of the drug [5]. The Biopharmaceutical Classification System divides drugs into four classes depending on drug product *in vitro* dissolution properties and *in vivo* bioavailability [6]. Poor dissolution of drug may be the rate limiting step to absorption and hence to bioavailability of drug. More than 40% of potent new APIs suffer from poor

solubility and thus pharmaceutical companies are interested in the amorphous state [7]. However, the higher bioavailability or absorption rate of the amorphous form of the drug may also cause problems. In 1980, the crystalline form of warfarin sodium was replaced by an amorphous form to reduce costs in hospital pharmacy. It increased the number of patients with a loss of anticoagulation control and overall health care costs [8]. Furthermore, the amorphous form has been observed to increase the skin permeation of ketotifen (antiallergy drug) compared with the crystalline form when a matrix patch is used [9].

In addition, many companies can gain patent protection for the amorphous form of a drug and a competitive advantage against other pharmaceutical companies. Pursuit of competitiveness is sometimes challenging because the amorphous state is a non-equilibrium state; an amorphous API may crystallise during storage or during a manufacturing process [10]. One of the world's best selling drugs, atorvastatin (Lipitor®) was formulated as an amorphous salt but it was observed to crystallise during phase III clinical trials [11]. This drawback delayed the launching of the drug onto the market a few years, and the total sales of Lipitor® were worth approximately $12.9 billion (USD) in the year 2006 [12]. There are several patents or methods for preparing amorphous atorvastatin from different salts by other drug companies. The new molecular API patent for atorvastatin is valid until 07-2011. Pfizer has also patented a process to prepare amorphous atorvastatin calcium, the same salt as in the crystalline Lipitor® on the market [13]. It may increase the patent protection time of Lipitor® because it is a different physical form of the drug.

In solid dosage form, other well known amorphous drugs with a low molecular weight are e.g. quinapril hydrochloride (Accupril®), zafirlukast (Accolate®), nelfinavir mesylate (Viracept®) and itraconazole (Sporanox®) [4]. In addition, nowadays there are many companies with products in the pipeline that are reported to be amorphous drugs with a low molecular weight. The future will show how many of these will come to market in an amorphous form.

Solid dispersions are one way to prepare a drug in an amorphous dosage form. There are a few commercial drug products on the market which are based on amorphous solid dispersion technology. These include Novartis's soft gelatine capsule Gris-PEG®, which is based on a solid dispersion of griseofulvin in polyethylene glycol (PEG 8000) [14]. Fujisawa's Prograf crème is based on a solid amorphous dispersion of tacrolimus in hydroxypropylmethylcellulose (HPMC) [15]. An amorphous drug product called Sporanox® is sold as hard gelatine capsules and is based on an itraconazole-HPMC solid dispersion which is coated onto sugar beads [16]. Lilly's capsule product Cesamet® is based on a solid dispersion of nabilone in povidone [14]. The newest amorphous dispersion sold as soft gelatine capsules, is Roche's Fortovase® containing saquinavir mesylate suspended in glycerides [17]. Many solid dispersions are sticky and thus processing into a solid dosage form is challenging due to stickiness [14].

The main objective of this study was to develop a processing method for a small molecular weight model material that has a glass transition below ambient temperature and is thus sticky. In addition, features of the material intended to increase the physical stability of a low molecular weight binary system are studied, including systems enhancing physical stability against crystallisation are discussed. The literature review is focused on the scientific literature of the amorphous state and patents for amorphous formulations that have been accepted world wide.

2. Literature review

2.1 Processing methods to produce amorphous material

The large scale preparation of an amorphous drug is a problem for the pharmaceutical industry at the moment [18]. In addition, there are problems in the methods of physical characterisation of the amorphous state, because the methods used are focused on observing the lack of crystallinity and not the presence of the amorphous state [18,19]. Some of the amorphous drug systems classified as amorphous may exists as a liquid crystals because of inadequate physical characterisation [20].

Several methods for the preparation of amorphous forms of drugs and chemicals have been described in the literature (Table 1). At the moment, the most common methods for large-scale production of amorphous material are freeze-drying, spray-drying and melt extrusion [19]. At the beginning of the new millennium it was approximated that about 8 of the 60 new chemical and biological entity solid dosage forms approved by the FDA were partially or completely amorphous and were prepared by freeze-drying [21]. One reason for the popularity of freeze-drying in production of amorphous materials is that the operation parameters can be easily controlled and measured. In addition, many pharmaceutical companies have the necessary instruments, and amorphous matrix has been observed to increase the chemical stability of proteins and peptides.

Usually, excipients are needed to stabilise and to improve processability of amorphous drug formulations. Quite a common method is to use a solid dispersion where the API is formulated into a matrix or a carrier [22]. Unfortunately, these formulations are often sticky and they need a great deal of excipients [14,23]. Extrusion methods are especially used to formulate solid dispersions, because chemical degradation can be reduced by controllable energy input during processing [19].

Phase changes during storage or processing may also change material to an amorphous form. Hydrated sodium celecoxib was found to transform from the crystalline hydrate form to an amorphous form during storage, which increased oral bioavailability [24]. Dehydration might be a quite useful method to produce amorphous material because it does not cause high physical stress on the material processed, as occurs in milling and melting methods. However, the utility of the dehydration method depends on the hydrate form of the drug because not all hydrates can form a pure amorphous material when dehydrated.

Table 1. *Methods to prepare amorphous materials.*

Method	Processing temperature		
Industrial scale	[°C]/ s, l *	Possible problems in processing method	Reference
Freeze-drying	< 0 °C / s	Many processing steps Consumes energy Slow and thus expensive Limited capacity Residual solvents	[3,25]
Spray-drying Spray-freezing	> 25 °C / l < 0 °C / l	High temperature (spray-drying) Many process parameters Energy consumption Residual solvents	[26-28]
Melt extrusion	> 25 °C / s, l	High temperature High amount of excipients/water are usually needed	[29]
Other methods	[°C]/ s, l *	Possible problems in processing method	Reference
Addition of impurities/isomers	approx. 25 °C / l	Not well studied at least with isomers	[30,31]
Melt quenching	> 25 °C / s	High temperature Cooling is usually needed Chemical degradation Energy consumption	[18,19,21,32, 33]
Precipitation by antisolvent addition	approx. 25 °C / l	Rapid addition of solvent Residual solvents Solubility problems if water is used	[33]
Dehydration of hydrated crystals	> 25 °C / s	Promising method Not suitable for all crystals	[34]
Mechanical stress (milling, grinding)	< 25 °C / s	Milling time dependence High temperature if cooling is not used Dependent on crystal structure Seed crystals remain in formulation	[35]
High pressure compaction	approx. 25 °C / s	Pressure from 0.1 to 5 GPa Energy consumption, Only suitable for small amounts of material	[36]
Electric field	approx. 25 °C / s	Not used for drugs Only tested for polymers	[37]
pH change	approx .25 °C / l	Residual solvents	[33]
Vapor deposition	> 25 °C / s	New method for drugs Materials prepared have extraordinary properties like physical stability Chemical degradation	[38]
Vacuum systems	> 25 °C / l	Residual solvents	[39,40]
Electrospinning	> 25 °C / l, s	Amorphous drug-polymer nanotubes Not a large scale production method	[41]
Ultrasound	approx. 25 °C/s, l	Cavitation Chemical degradation Not tested for drugs	[42,43]

* Starting material at the beginning of the process, s, solid and l, liquid.

Processing method has an effect on the physical and chemical stability of the amorphous state. Patterson and co-authors (2005) compared ball milling and quench cooling of four different pharmaceutical drugs: dipyridamole, carbamazepine, glibenclamide and indomethacin [35]. Quench cooling was observed to be a more effective method to prepare physically stable amorphous form than ball milling, but it may induce chemical degradation. Production of an amorphous form by ball milling is dependent on the unit cell structure of the crystalline drug. Vacuum/film drying was found to produce physically more stable amorphous material than freeze-drying or spray-drying [40]. Stability properties differ across drug substances because of changes in the physical properties of drugs. In addition, processing parameters such as the spraying temperature (inlet-outlet temperature) in spray-drying have been found to have an effect on the physical stability of amorphous form although the glass transition and infrared spectra of materials were similar [44]. This result was related to the degree of disorder in the amorphous materials, which depended upon the processing temperature. According to Shalaev and Zografi (2002), changes in processing parameters produce different kinetic states for amorphous materials [45], which may have effect on physical/chemical stability.

2.2 Properties of the amorphous state

2.2.1 Glass transition

The glass transition temperature (T_g) is the most important parameter of an amorphous material [46]. The nature of a glass and T_g is considered to be the most interesting unsolved problems within solid state science [47]. There are many theories for glass transition, but they are reviewed elsewhere (in e.g. [1]). Glass transition is observed when an amorphous solid (glass) changes into a supercooled liquid state during heating or to the reverse during sample cooling (Figs. 1 and 2).

A schematic representation of the difference between the glass transition (T_g) of an amorphous material and melting (T_m) of a crystalline material is shown in Fig. 1. T_g is thought to be approximately 2/3 of the melting temperature [48]. In principle, all fluids or melts can be turned into amorphous glass if the cooling rate is rapid enough and the material does not crystallise during cooling [49]. Glass transition is a kinetically controlled phenomenon and thus different cooling rates have effect on T_g (Fig. 1) [50]. Upon cooling melt can enter a supercooled liquid state if the melt does not crystallise at temperatures below melting point. During cooling the viscosity increases and the material starts to solidify forming a glass at temperature below T_g. Upon cooling there is also observed change in thermodynamic properties such as volume, enthalpy and entropy (Fig. 1). The Kauzmann

temperature (T_k) is a hypothetical temperature where the molecular rearrangement approaches a minimum value i.e. equal to that of the crystal [48]. It can be extrapolated from the thermodynamic properties such as volume, enthalpy or entropy.

Glass transition involves changes in molecular motion. The structural relaxation time (τ) is used to evaluate molecular mobility in the amorphous state. At T_g, τ is about 100 s, and much less at temperatures above T_g [51]. Molecular motions are restricted in a glassy state to vibrations, stretching and short-range rotational motions.

Glass transition is associated as α relaxation, where molecules may have translational motions. At temperatures below T_g, there are also other relaxations called β, γ, … relaxations, with decreasing transition temperatures. The magnitudes of those other β, γ relaxations are much smaller than α relaxation. The origin of β and γ relaxations are still unclear for small molecules, but in large molecules such as polymers it has been stated that these relaxations are local mode relaxations in the polymer chain and the rotations of terminal groups and side chains [46]. Above T_g, molecules may have translational movement. These higher molecular motions are restricted to small regions (15%, V/V) surrounded by less mobile fractions [52]. It has also been proposed that molecules move a distance of 20% of the molecular diameter at temperatures near the T_g [53].

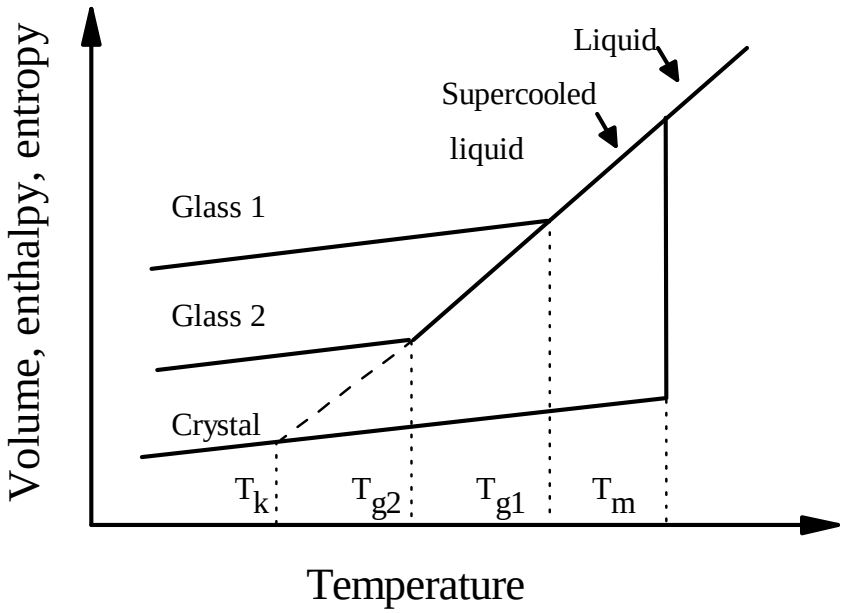

Figure 1 *A schematic representation of changes in entropy, enthalpy and volume as a function of temperature for a material that can be in the crystalline or amorphous state. Glass 1 is cooled down more rapidly than Glass 2. Kauzmann temperature (T_k); glass transition temperature (T_g); melting temperature (T_m) of the crystalline material. Modified from Ediger and co-authors (1996) [51].*

Physical changes in the glass transition can be studied using different instrumental methods [32,54-56] (Fig. 2). The material is sticky and more elastic at temperatures above the T_g than at lower temperatures. Stickiness decrease the processability of the material and there can be some problems in storage of amorphous pharmaceuticals. An increase in molecular mobility and reduction in the viscosity of an amorphous material has time-dependent structural changes in material properties such as crystallisation, stickiness and collapse of material structure [1,56,57]. In addition, increased diffusion, rates of enzymatic reactions, the Maillard reaction and oxidation are related to the glass transition [58]. Reaction rates are dependent on the temperature difference $T_{ambient}$-T_g.

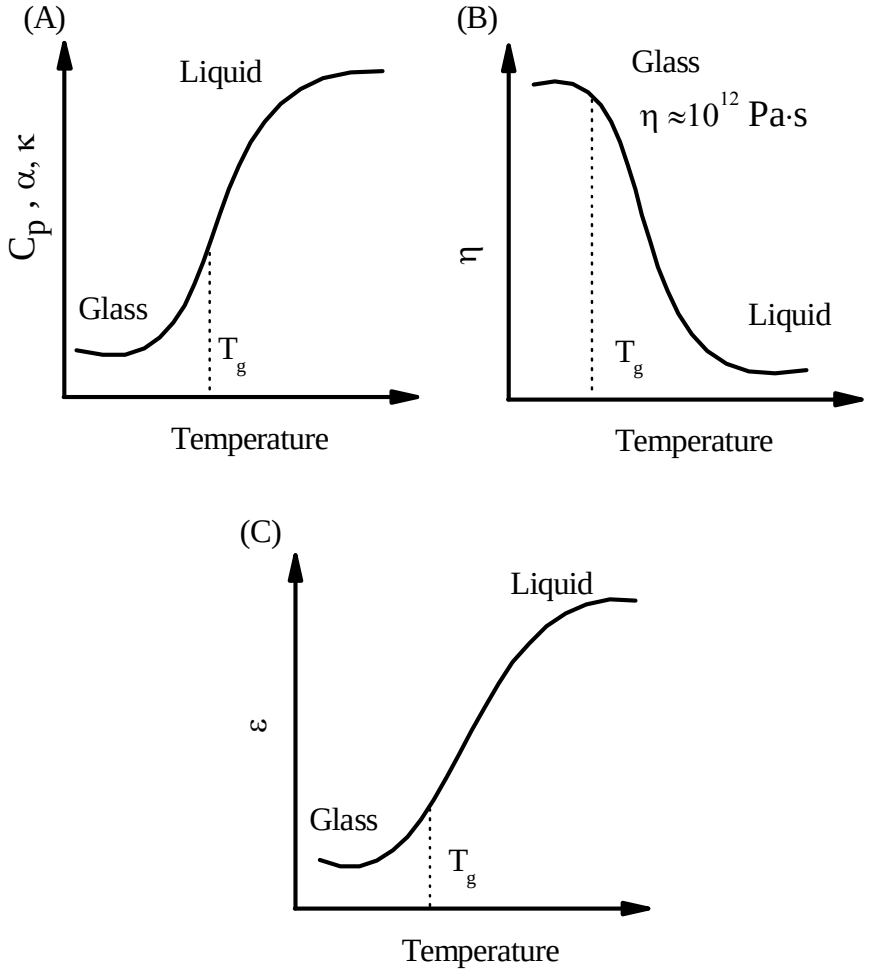

Figure 2 *Changes in physical properties during the glass-liquid transition (T_g). (A) Coefficient of expansion (α), isobaric expansivity (κ), isobaric heat capacity (C_p), (B) viscosity (η), and (C) dielectric constant. Modified from White and Cakebread (1966) [56].*

2.2.2 Physical aging

Physical aging is a structural relaxation towards thermodynamic equilibrium as a function of time [59]. Annealing and physical aging are often used as synonyms in the literature. Physical aging is observed at temperatures below T_g in the non-equilibrium state, and it occurs at a constant temperature at zero stress without any external input. A schematic presentation of the physical aging of glass A to glass B during annealing time (t_1) is presented in Fig. 3. At low temperatures, new apparent equilibrium is difficult to achieve because molecular mobility is low and thus the time scale for observing physical aging is long [59]. Different apparent equilibria exist below T_g depending on thermal history and processing of the amorphous material. At temperatures above T_g, physical aging is not observed because molecular mobility and thus molecular rearrangement occurs so quickly that equilibrium is achieved rapidly.

A thermodynamic driving force drives an amorphous material towards the crystalline state during annealing. Another reason for physical aging is molecular motion that still happens at a lower temperature than T_g but over a longer time than in the liquid state. The molecular relaxation time (τ) increases as the glass relaxation progresses [60]. Thus, physical aging experiments will take time.

Reversible changes in enthalpy, specific volume, mechanical, spectroscopic and dielectric properties can be used for the detection of physical aging. The most widely used method is DSC, where an endotherm is recorded at or near T_g due to physical aging.

In materials science, it has been found that more compact molecular order and strengthened molecular interactions change the physical properties of the amorphous material, such as mechanical and diffusional properties due to annealing [61]. Physical aging decreases water vapour sorption in amorphous systems [62]. Thus, sorption properties are dependent on time, because structural transformations and phase transitions may have an effect on sorption [1]. Physical aging is observed to have an effect on the density, brittleness, and compaction properties of polymer materials [63-67]. Hence, annealing has gained considerable attention during the past few years. In addition, amorphous materials often crystallise during aging [68]. Physical aging also increases ultrasound attenuation in polymers and thus physical aging has an effect on ultrasound processing [69].

Controlled annealing has been observed to increase the chemical stability of amorphous systems compared with non-annealed materials [70]. This might be related to lower molecular mobility in the annealed material. Pfizer has patented a method in which annealing is used to improve the chemical stability of amorphous materials by different annealing methods such as temperature, pressure, microwaves and ultrasound [71,72]. Annealing was found to decrease the degradation rate of amorphous material in longterm storage [72]. Because different processing conditions, parameters and

equipment produce glasses of different kinds, controlled annealing might be one solution to solve problems with interbatch variation.

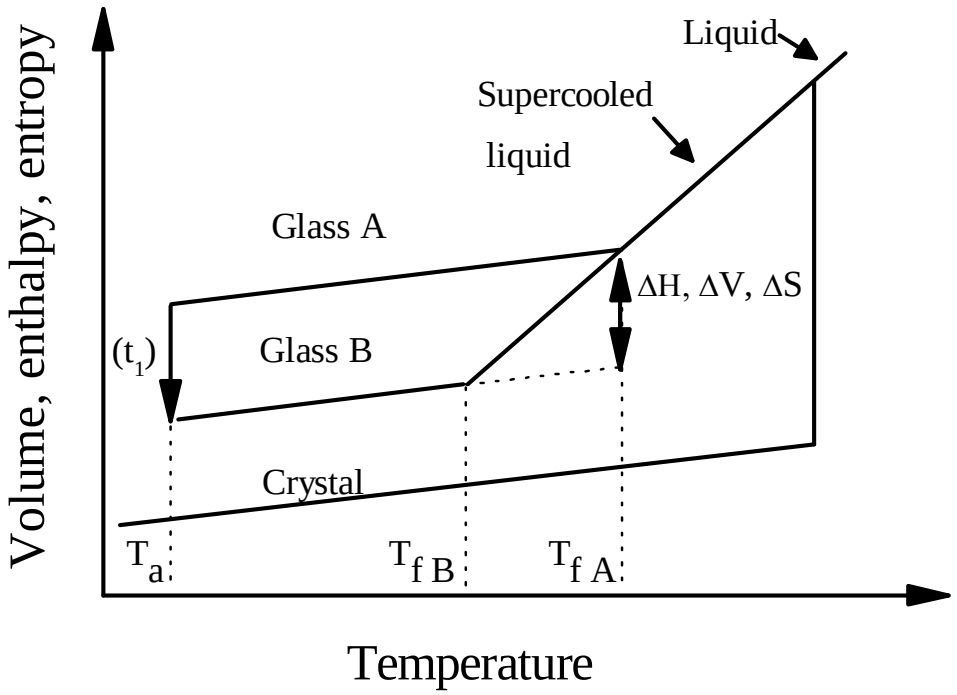

Figure 3 *A schematic representation of physical aging of glass A to glass B during aging time (t_1) at annealing temperature (T_a). Fictive temperature (T_f) is the temperature where the structure of the glass ($T_{f\ A}$ or $T_{f\ B}$) is fully relaxed. Crystals are stable against annealing. Modified from Hancock and others (1995) [73].*

2.3 Factors affecting physical stability of the amorphous state

The physical stability of amorphous material against crystallisation is reviewed. The dissolution rate of a drug decreases when the material is transformed from the amorphous state to the crystalline state. Thus, the pharmaceutical industry and many researchers are studying different methods to stabilise amorphous drugs. Today, there are two different views in the literature concerning what are the main factors for physical stabilisation of the amorphous state. They are: (1) interactions between molecules or (2) molecular mobility. However, molecular interactions and molecular mobility are usually interrelated. In addition to these two, there are many other factors considered to be important, and thus these different factors are reviewed, some of them are also related to molecular interactions

and molecular mobility. Inhibition of crystallisation is being affected by more than one factor [74].

2.3.1 Molecular interactions

According to Ovshinsky (1985), the first rule of non-crystalline solids is that atoms have bonding options, and the second rule is steric hindrance [75]. Steric hindrance prevents molecules from making contact with each other and thus the desired atomic and molecular arrangements for forming a crystal lattice. Such obstacles to molecular motion can be crosslinks and bridges, which prevent crystallisation.

Hydrogen bonding plays a crucial role in the stabilization of organic structures [76]. Similarly, the crystallisation tendency of drugs has been explained by differences in hydrogen bonding, steric structure and symmetry [77]. Having many possibilities for forming hydrogen bonds between different acceptors and donors makes the crystallisation of molecules more difficult [4,78] due to possible mismatches in hydrogen bonds.

An interaction model explains formation of a non-crystalline state by the disruption of specific drug-drug interactions or by the formation of specific drug-excipient interactions. In network glasses, crystallisation is prevented by directional bonds that inhibit the formation of long range order [79] and it has been proposed that, in the sugar glasses, hydrogen bonds act as a network [80]. However, there are studies which have reported that hydrogen bonding is not needed to stabilise an amorphous drug [81].

There might also be some cooperative interactions in amorphous materials. Hydrogen bonding is reported to decrease polymer chain mobilisation and thus has an effect on measured T_g. T_g of a thin polymer film was found to decrease with decreasing film thickness on a gold surface [82]. This was explained by the decreased cooperativity of molecules in the thin film and lack of interactions between the gold and polymer layer. The T_g of a film increased with decreasing film thickness on silicon oxide, and it was postulated that weak hydrogen bonding to silicon might have increased the T_g. Similarly, for amorphous drugs, such as indomethacin and celecoxib, milled materials crystallised more easily than unmilled materials [83,84]. It is more likely that the milling processing of these drugs triggered crystallisation than the decreased cooperativity between molecules. Furthermore, the crystallisation of small glass forming molecules is found to start at interfaces [85].

Specific understanding of interactions between excipients and proteins/peptides/drugs is a key factor for further development of pharmaceutical processes such as freeze-drying because these interactions may vary from protein to protein [86] and thus a clear rule of thumb for physical stabilisation of amorphous forms has not been developed yet.

2.3.2 Molecular mobility

Molecular mobility has been found to be related to the chemical and physical stability of drugs [73,87,88] and even to microbial responses in foods [89]. Molecular mobility is thought to predict the shelf life of an amorphous pharmaceutical product. The practical storage temperature of an amorphous material is proposed to be 50 °C lower than the T_g, because molecular mobility is assumed to be so low at these temperatures that it has a minor effect on physical stability [73]. This temperature is quite near the T_k (Kauzmann temperature) where molecular mobility vanishes. However, crystallisation is reported to occur at 175 °C below the T_g [90], although the maximum crystallisation rate is reported to occur between T_g and T_m [54,91]. At temperatures below T_g, molecular motion is too slow for crystallisation. At temperatures higher than the T_m, thermodynamic equilibrium is shifted to the liquid state preventing crystallisation. Crystallisation is dependent not only on temperature but also on aging time [92].

The structural relaxation time (τ) is used to estimate molecular mobility in amorphous materials. Nowadays, the methods for measurement of τ are mainly thermal methods, for example DSC, or more often solid-state NMR (ssNMR). The relaxation time is frequently correlated with the shelf life of the amorphous product and thus molecular mobility is studied widely. However, there are still many theoretical and practical limitations to the use of molecular mobility concepts to predict the chemical and physical stability of an amorphous material, such as accuracy of measurements [93]. There is also need to develop theories to explain role of molecular mobility on physical stability.

In the literature, there are many methods to describe molecular relaxation times (τ). The Kohlrausch-Williams-Watts (KWW) equation (Eq. 1) is widely used to define the mean relaxation time distribution constant (β) and mean molecular relaxation time constant (τ^{kww}) using the extent of relaxation (ϕ). In enthalpy recovery experiments using DSC [73], an amorphous material is stored for different times (t) at a temperature (T_A) below the T_g to observe enthalpy recovery (ΔH) in the DSC scan. Maximum enthalpy recovery (ΔH_∞) is calculated using Equation 2 (Eq. 2) where the measured heat capacity change (ΔC_p) at T_g is used.

(1) $$\phi = 1 - \left(\frac{\Delta H}{\Delta H_\infty} \right) = \exp\left[-\left(\frac{t}{\tau^{kww}} \right)^{\beta} \right]$$

(2) $$\Delta H_\infty = (T_g - T_A)\,\Delta C_p$$

The Adam-Gibbs-Vogel (AGV) theory describes glass relaxation controlled by configurational entropy and activation energy [94] and it is often

presented as in Equation 3 (Eq. 3) [95]. Because the KWW equation only describes the average for τ, a method for calculating the time-dependence of molecular mobility has been described [60]. The fictive temperature (T_f) is calculated as in Equation 4 (Eq. 4) which is combined with the normal AGV function (Eq. 3). A parameter γ is related to the ratio of C_p of the crystalline and glassy materials at T_g. The superscripts of C_p are liquid (l), glass (g) and crystal (c). The initial relaxation time (τ^0) of newly prepared glass can be calculated as shown in Equation 5 (Eq. 5) [93].

(3) $$\tau = \tau_0 \exp\left(\frac{DT_0}{T\left(1-\frac{T_0}{T_f}\right)}\right)$$

(4) $$T_f = T_f^0 \exp\left(-\frac{\gamma \cdot \Delta H}{\Delta C_p \cdot T_g}\right),\ T_f^0 = T_g^\gamma \cdot T_A^{(1-\gamma)}$$

(5) $$\tau^0 = \tau_0 \exp\left(\frac{DT_0}{T - T_0\left(\frac{T}{T_g}\right)^\gamma}\right),\ \gamma = \left(\frac{C_p^l - C_p^g}{C_p^l - C_p^c}\right)_{T_g}$$

The Vogel-Tamman-Fulcher (VTF) equation (Eq. 6) describes non-Arrhenius temperature dependence of the relaxation of a glass forming liquid i.e. a supercooled liquid. The temperature T_0 corresponds to the ideal glass transition temperature where relaxation times approach infinity and it is typically quite near the T_k. The "parameter of strength" (D), indicates deviation from Arrhenius' law and it describes the fragility of the liquid. For fragile liquids, D would be below 10 and 30 to infinity for very strong liquids [96-98]. τ_0 is the pre-exponential factor, being usually of a similar order of magnitude as vibrational lifetimes (i.e. 10^{-14} s). Fragility (D and T_0) parameters can be determined using the Vogel-Tamman-Fulcher (VTF) equation from the viscosity data, because viscosity (η) is related to molecular relaxation time (τ). Crowley and Zografi (2001) have described how to evaluate fragility parameters using thermal methods [97].

(6) $$\tau = \tau_0 e^{\frac{DT_0}{T-T_0}}$$

2.3.3 Other factors affecting physical stability

Development of blends with high T_g, which is related to molecular mobility, is one of the most commonly used methods for increasing the physical stability of amorphous materials. Quite often polymers are used to increase T_g [99] due to their antiplasticising capability. However, it seems that the effectiveness of the additive for preventing crystallisation is not directly linked to the change in T_g [100]. Mixing amorphous drugs with a polymer has also been found to decrease the free volume of the system [101] and thus increase the physical stability. Other factors favouring the formation of the glassy state are: a high viscosity in the liquid just above the solidification point, a rapid rate of cooling, a complex molecular structure and the presence of more than one molecular species in the system [56,102]. Purification during large-scale manufacturing of a new amorphous API may produce problems. The first batch produced at the beginning of the development of a new API contains more impurities than production scale batches. Thus a metastable form may crystallise in the production scale batches due to lowered impurity level [31]. Isomers of drugs/excipients can also be used to stabilise the amorphous state as in, for example, mannitol-sorbitol binary mixtures [30].

In biological materials addition of some other components such as salts [103] and surfactants [104] stabilise chemically amorphous systems during freeze-drying. The mechanism of stabilization is still unclear. Complex formation between salts and sugars is thought to be one reason for the increased chemical stabilisation [105,106]. Ranbaxy laboratories has patented a method where less than 5% (w/w) of alkali metal salts has been added into amorphous atorvastatin formulation and it has been observed to increase the chemical stability of the drug [107]. Surfactants are assumed to change the interface between different phases [104]. These factors may also have an influence on physical stability of freeze-dried systems.

The benzene ring is believed to act as a steric hindrance in m-toluidine glass that restricts the hydrogen bond network from growing in a single direction [108]. Aromatic rings and rings with other electron donating groups are thought to stabilize intermolecular interactions such as dipole forces in the amorphous state [109].

Large and heavy halogen atoms are found to disturb molecular crystal packing and diffusion of molecules in the crystallisation process, favouring glass formation [110]. Crystallisation tendency of halogenated compounds increased in the following order: F<<Cl<Br. Similarly, T_g decreased in the following order Br > Cl > F (T_g from 54 °C to 72 °C) and T_m decreased in the following order F > Cl > Br. The bulkier and heavier halogen substituents were thought to disturb diffusion and packing of molecules. In drug molecules, the form of a salt has been observed to change the T_g of indomethacin (free indomethacin T_g 42 °C) from 69 °C to 139 °C due to changes in electrostatic interactions between the carboxylic acid and the

alkali salt [111]. This is an interesting finding because pharmaceutical drugs often have halogen substituents or different salt forms.

Hydrogen ion activity (pH) is known to be important in the liquid state for the chemical stability and properties of a molecule. However, in the solid state the effect of hydrogen ion activity is still unclear [3]. Solid-state pH has been postulated to have an effect on the chemical and physical stability of an amorphous system [112,113] and it has also an effect on preparation of amorphous or crystalline drug from the solution [114]. Still, there is a problem of how to measure solid-state pH in a reliable way. The devitrification kinetics of amorphous irbesartan (weak acid, pKa is approximately 4.9) have been observed to be slower in acidic conditions than in pure water [115]. Thus, it might be that the drug release site in the human body (pH) might have an effect on the bioavailability of an amorphous drug, although the apparent dissolution rate of an amorphous drug should be good.

An amorphous system is thermodynamically in a non-equilibrium state and thus it tries to achieve an energetically more stable crystal form. Thermodynamic properties are believed to be the driving force for the crystallisation of amorphous material [116-118] and they are thought to be more dominant mechanisms in crystallisation of amorphous material than molecular mobility [117]. Such thermodynamic properties as configurational entropy [118], differences in free energy (enthalpy and entropy) [117] and the kinetic barrier for crystallisation [116] are considered to be important for approximating the crystallisation tendency of drugs.

In the solid dispersions, physical stability is related to the crystallisation tendency of the pure amorphous drug [119]. Thus, drug properties also have an effect on the physical stability of dispersions. The amorphous state has been found to be physically more stable within drugs with a complex molecular structure. The conformational flexibility of molecules allows development of more stable amorphous drugs and thus the number of amorphous drugs on the market has increased [4,78,102,120]. Low structural symmetry and a bulkier structure are also known to be important inhibitors of crystallisation [121].

2.4 Stickiness

A material appears sticky when it has a tendency to adhere to a contact surface. The stickiness of amorphous materials causes problems in processing which can be operational problems, material losses, agglomeration and clumping [122,123]. Sticking to fingers and packaging increase also customers' dissatisfaction [123].

2.4.1 Theories of adhesion

Adhesion happens between two different surfaces. Cohesion is formed between two similar surfaces. Both phenomena are a result of forces between molecules [124]. Present theories are not describing in detail all the interactions that occur during adhesion and what the primary forces involved are. The forces operating in adhesion and cohesion are van der Waals forces (physical adsorption), hydrogen bonding (strong polar attraction), ionic, covalent or chemisorption forces. Van der Waals and electrostatic forces are primary factors for adhesion whereas chemisorption or covalent bonding much less commonly play a role [125].

The theory of adsorption assumes that adhesion is the result of molecular contact between two materials, causing surface forces to develope. A good contact requires that the separation of surfaces should be less than five Ångströms, which means good wetting between the surfaces. There should not be air pockets along the interface and the wetting should be complete. Thus, when good wetting is desired, the surface energy of the surface (γ_s) must be high and the surface tension of the wetting liquid (γ_l) must be low i.e. $\gamma_s >> \gamma_l$ [124].

In the *mechanical theory* of the adhesion, the adhesive has to penetrate the cavities of the substrate [124]. Increasing the surface roughness assists mechanical anchoring because it may increase interlocking, the formation of a clean and reactive surface or surface area. The mechanical theory also explains the main adhesion mechanism for a porous material. It requires that the adhesive displaces trapped air to get good contact. There may also be *liquid bridges* between surfaces [126]. *Electrostatic forces* are important for adhesion between electrical double layers. This concept is widely used in biological cell adhesion [124]. The *diffusion mechanism* is possible for large molecules like polymers, for instance. It requires that polymer molecules are capable of moving. Polymers are diffused between each other and this induces entanglement and thus adhesion [124].

In the *weak boundary layer mechanism*, in order to get a good contact between adherend and surface other weak boundary layers such as air and water must be removed. This means that when adhesion fails, it is the result of failure of a weak boundary layer, not a failure of an adhesive surface. Thus, adhesion is the result of the combination of environment, adhesive and surface. Again, surface treatment is important in order to remove any weak-boundary layer.

The suction cup theory was created because van der Waals forces are a ten-thousandth of the force exerted by an adhesive tape [127]. The s*uction cup theory* is related to air bubbles on rough surfaces that lead to a suction effect when attemting to remove the adhesive [128]. This suction effect keeps the adhesive stuck to the surface.

2.4.2 Factors causing stickiness

Several factors have been implicated in stickiness (Table 2). Factors increasing stickiness are hygroscopicity, solubility, low melting point, viscosity, temperature, mechanical stress, excipients and particle size [123,129,130]. In addition, long contact time increases caking and stickiness even if all the other factors are the same [131]. When the viscosity of an amorphous material decreases rapidly, it causes stickiness. The critical viscosity incurring stickiness and caking was found to be approximately 10^7 Pa·s [132]. Viscosity can be related to relaxation times above the glass transition temperature [46].

Table 2. *Factors causing stickiness and their relative contribution. Negligible contribution (0), high contribution (+), higher contribution (++), the highest contribution (+++). Modified from Adhikari and co-authors (2001) [123].*

Factors	Relative contribution to stickiness	Reference
Protein	0	[123]
Polysaccahrides	0	[123]
Fats	+	[123]
Particle size distribution	+	[123,125]
Low molecular weight sugars	++	[123]
Organic acids	++	[123]
Compression/ pressure	++	[123]
Water/ relative humidity	+++	[123,133]
Temperature	+++	[123]
Viscosity	+++	[123]
Some other factors	**Relative contribution to stickiness**	**Reference**
Glass transition temperature	+++	[124,134]
Solubility	+++	[124]
Surface free energy	+++	[124,132]
Contact time	+++	[132]

The chemical properties of a material, such as polarity and surface properties i.e. the surface energy, have an effect on wetting. The important factor for adhesion is that the adhesive should be able to flow on a molecular level to grip surfaces [124]. In two-phase systems, solubility parameters

between components are important because the difference in solubility may disturb bonding due to phase separation.

An increase in temperature over the T_g increases the molecular mobility and therefore the material can deform more easily under stress. In addition, the number of contacts between molecules increases as the molecular mobility increases and thus the adhesion is more elastic. A high molecular weight usually increases cohesion but decreases adhesion. High temperature and humidity favour caking of soluble materials especially if the melting point of the material is low. Crystallinity, molecular weight and polymer crosslinking decrease molecular mobility and thus decrease the adhesion bond strength against stress, while increasing cohesion [124]. In addition, an extended contact time increases caking and stickiness, even if all other factors are the same [57].

In Figure 4, the effect of temperature on stickiness as a function of water content is shown. A sticky region has an upper and lower limit depending on the viscosity. The temperature or water content will plasticize the amorphous material, inducing stickiness. At temperatures above T_g, material is changed from a glassy to a supercooled liquid state, which may cause stickiness [54,57]. The sticky point of amorphous sugars is from 10 to 20 °C higher than the glass transition temperature [57,134]. Viscosity in this temperature range changes from 10^6 to 10^8 Pa·s [132]. The sticky-point of skim milk is from 4 to 23 °C higher than the T_g [135]. If the product temperature is lower than the T_g, stickiness and adhesion will not take place [57].

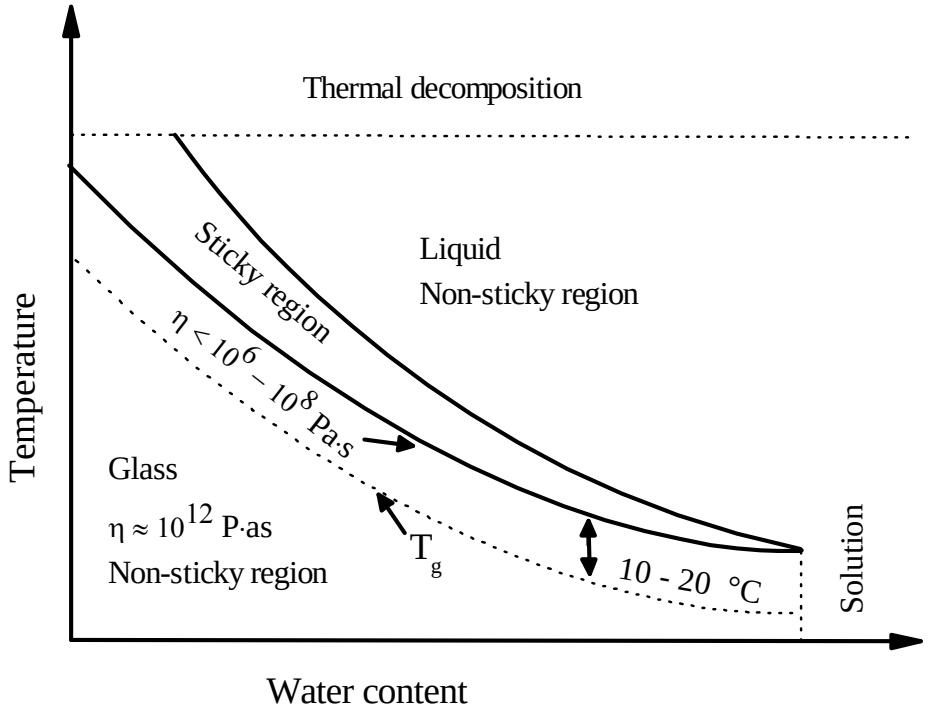

Figure 4 *Effect of temperature, water content, viscosity and glass transition temperature on the sticky region. Modified from Roos (1995) [1].*

2.5 Processing amorphous or sticky material into a solid dosage form

Powder stickiness is a problem when material with a low T_g is processed into a solid dosage form. Stickiness induces problems in processing of solid dosage forms if nothing else because authority requirements are high in the European Pharmacopoiea for Uniformity of Dosage Units (European Pharmacopoeia 6.0, 2.9.40) and stickiness interferes with uniformity. Lowering of temperature and water content are the first methods in the prevention of caking and stickiness of amorphous material [61]. In addition, many other formulations, such as solid dispersions, have processing problems because they are usually sticky and hygroscopic [23]. To prepare a solid dosage form from sticky material is possible but it requires huge amount of excipients. Preparation of a 25 mg indomethacin solid dispersion tablet requires approximately 600 mg excipients, for instance [14]. In this literature survey, some possible processing methods for sticky material are introduced. However, many processing methods may cause crystallisation of amorphous material during processing [136].

2.5.1 Temperature and water content

Low temperature and water content increase the viscosity of amorphous material and thus decrease stickiness during processing (Fig. 4). Another technique to process the material at high temperature, where amorphous material behaves like a liquid, and use it to fill capsules, for instance [137]. This processing technique might have some drawbacks because some amorphous material might start to degrade or crystallise at the temperatures needed to decrease viscosity. Thus, low temperature processing is an important method in the processing of sticky material.

In low temperature processing, it is important to control the temperature of the wall in contact with the material. One way is to use cold air or some other cooling system in the bottom of the processing chamber [123]. In addition, mechanical scrappers are used to decrease the mass stickiness on the walls. One problem with cold air is the condensation of water on the chamber wall if the processing is done in ambient conditions. The problem of water condensation can be solved by using free flowing nitrogen gas in the chamber or some other inert gas. For cryogenic processing (i.e. the use of dry ice, liquid carbon dioxide or liquid nitrogen) the problems are high operation costs and high energy consumption [138]. The cost of liquid nitrogen is approximately 43% of the total costs of the industrial scale system [139]. After cryogenic processing, further processing of a solid dosage form requires low temperature facilities/rooms to inhibit stickiness. Thus, some other techniques are more realistic and cheaper to use for industry than cryogenic processing.

2.5.2 Antiplasticizer

Amorphous material can be plasticized thermally and using plasticizers. Plasticizer is usually a liquid e.g. water or other small molecular weight molecule acting as a lubricant in the blend. Thus, antiplasticizers are used to increase T_g or absorb/adsorb water. Water drastically decreases the T_g of amorphous material and only a small amount of water may cause a significant decrease [54]. One type of antiplasticizer used is a porous antiplasticizer which competes for available water [140]. This is due to the fact that excipients will protect an amorphous drug from moisture [141,142]. Good water sorption of residual water by the amorphous excipient might be one reason why amorphous excipient is a good chemical stabilizer for protein formulation in freeze drying [143]. Usually in amorphous drug formulations microcrystalline cellulose, starch, sugars and silicone dioxide are used as water sorbents.

Some other antiplasticizers (e.g. silicone dioxide) interfere with liquid bridging, decrease friction, reduce molecular attractive forces and inhibit crystal growth [140]. High molecular weight sugars and starch derivatives are used to increase T_g and thus can be successful in decreasing stickiness in food products [144]. Maltodextrins have been used to aid drying, thereby minimising stickiness and caking during spray-drying because they increase T_g. Common sugars such as fructose and sucrose have low T_g's [131]. The effect of ingredients on T_g is predicted by the Gordon-Taylor, Couchman-Karasz or Huang equations in multiple systems [1]. It might be that T_g is not the only factor responsible for stickiness, because the surface properties of dried materials, such as porosity are also important. Lipids may reduce caking by forming a water-protective barrier [130].

2.5.3 Drying methods

Nowadays glassy pharmaceutical products are processed mainly by drying (Fig. 5, Table 1). Sublimation is used in a freeze-drying process where the solution of excipients and an active pharmaceutical ingredient (API) is dried under suitable conditions. The freeze-drying process is slow in comparison with spray-drying and it also requires high amounts of energy. In spray-drying and chilling the solution is sprayed into a warm or cooled chamber, respectively. Spray-drying is more common due to simultaneous drying in the chamber, whereas chilling needs a separate drying step after spraying, if solvent is used. These processes produce amorphous form due to rapid liquid evaporation or solidification. Spraying can be difficult due to stickiness and it requires a substantial amount of drying aids, which increase the size of the solid dosage form [145]. Sometimes processed material might still be sticky after drying and thus difficult to process further into solid dosage form.

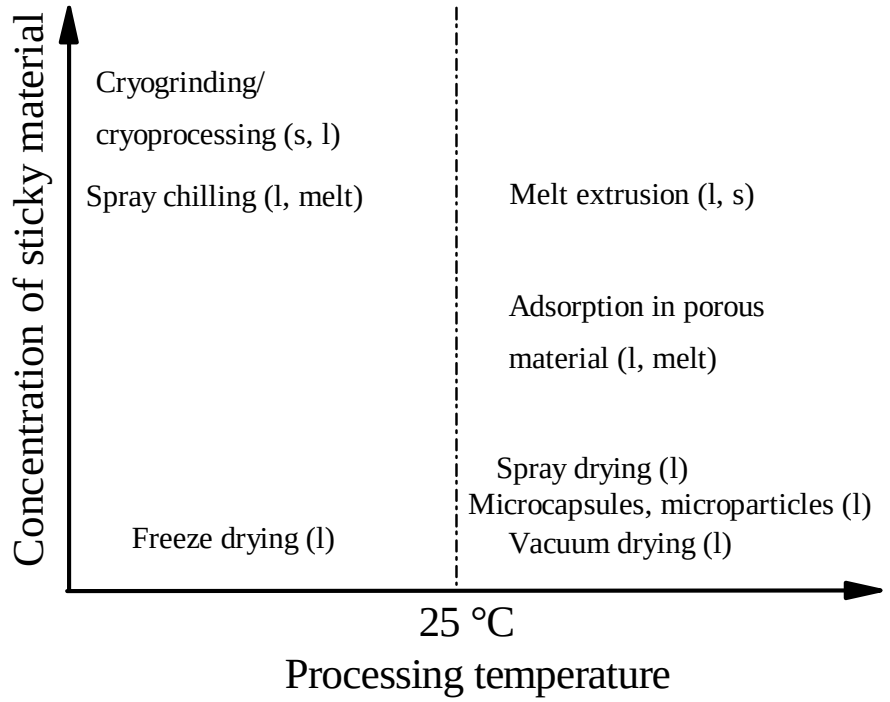

Figure 5 *Different ways of processing sticky substance into a solid dosage form. Concentration of sticky material in the beginning of the process as a function of processing temperature. Concentration will change depending on the physical form of the sticky material, l, is liquid,and s, is solid, or melt.*

2.5.4 Dispersions

There has been active research within the solid dispersion field but usually there are problems with scale-up and chemical or physical stability, explaining why there are only a few solid dispersions on the market today [14,146]. Solid dispersions can be used for processing of sticky substance and they can be further processed into different solid dosage forms such as soft/hard capsules, tablets and granules depending on the excipients.

Karrlsson and co-authors formulated greasy/oily/sticky substances into solid polymeric matrices [147]. The amount of drug in the beads varied from 15% to 70% (w/w). Chiesi and Pavesi (1991) mixed oil/ triglycerides or soya lecithin with ipriflavone to produce a dispersion [148]. The dispersions were enclosed in soft gelatin capsules. The amount of ipriflavone in capsules was 50% (w/w) of the total mass. Yanai and colleagues (1997) made a dispersion of API in an oleaginous base [149]. The dispersion was a liquid or a solid depending on the quality of the oleaginous base. The amount of API varied from 25% to 50% (w/w) in solid- or liquid dispersion, respectively. A similar method has been used in dosing of HIV protease inhibitors [17]. The size of

the dosage form was huge because 200 mg of API needed approximately 800 mg of glycerides. The large size makes these formulations difficult to swallow. In various lipid-based vehicle formulations, maximum drug loading varies from approximately 30% to 40% (w/w) [150].

2.5.5 Melt extrusion

Because the melt extrusion process cannot be used for a pure drug substance, it is quite often used to prepare solid dispersions having carriers in the formulation. Melt extruded materials can be used to make capsules and tablets. Breitenbach and his colleagues (1995) used water soluble PVP and starch derivatives in the melt extrusion of drugs, vitamins and amino acids [151]. The maximum amount of model substance could be 60% (w/w) depending on the drug properties. The processing temperatures of extruders usually range from 60 °C to 150 °C. High temperatures may increase degradation of the API during processing. The melt extrusion method has also been used for liquids (melts and solutions) where the maximum liquid load was approximately 40% (w/w) [152].

2.5.6 Loading into a porous structure

Loading into/onto a porous structure is a common method for processing oily and sticky substance. Quite often oil and oil soluble substances are loaded into natural polymers, such as materials derived from starch, dextrin or gum, by spray-drying. In an adsorption test, agglomeration of adsorbent started when 41% (w/w) of light mineral oil was added [153]. Total sorption (i.e. glimmering of the surface) of light mineral oil on a natural polymer was 334.9% (w/w). Natural polymers are observed to be good adsorbents/absorbents because they usually adsorb/absorb more material/oil into/onto themselves than magnesium carbonate does, for instance. Furthermore, adsorption of emulsions onto silica particles is possible [154]. Adsorbed/absorbed particles can be further processed with different drying methods, as described by Breton and co-authors (freeze-drying/spray-drying) [154]. Again, the size of this preparation might be too big if a relatively high amount of API is needed in a single dosage form.

2.5.7 Microcapsules and microparticles

Microcapsules and particles can be processed into a solid dosage form. Microcapsulation is a rather slow and complicated process. Perrier and Buffevant (1993) introduced polysaccharide microcapsules and microspheres for food, cosmetic and pharmaceutical ingredients [155] but also some other

materials can be used to form microparticles. It was possible to capsulate oily, liposoluble, water soluble and non-soluble particles. The drug loading in these microcapsules was approximately 40% (w/w) (o/w emulsion). Calcium gluconate for the preparation of fatty acid microparticles has also been used where the mixture of ingredients is dried and pulverized [156]. The amount of calcium gluconate was preferably from 50% to 90% (w/w) in these microparticles. Kumabe patented in 1999 a method for encapsulating oily, oil soluble and water soluble substances in a calcium microparticles [157].

2.6 Ultrasound processing

2.6.1 Principles

The definition of ultrasound is a pressure wave oscillating at a frequency above human hearing, i.e. above approximately 20 kHz (Fig. 6). Ultrasound processing is done without high forces and large displacements [158]. An ultrasonic apparatus consists of an electromechanical transducer, which usually is made of the piezoelectric ceramic of lead zirconate titanate due to its electromechanical conversion efficiency. Typically, conversion efficiency is 95% or more [158]. It is a non-contact method and it can be sealed outside the operation vessel. Thus, ultrasound can also be used in instrumentation where frequencies vary from 20 kHz in gases to 10 MHz in solids [159]. Intensities used in ultrasonic cleaning baths are approx. 1 W/cm^2, and in laboratory scale sonochemistry, intensities varies from 50 to 500 W/cm^2 [42]. Power levels in low intensity ultrasound are less than 1 W/cm^2 and thus no physical or chemical reactions in materials are detected [160]. Ultrasound cannot travel in a vacuum because it is a pressure wave. Effects on materials are cavitation and microstreaming in liquids. Cavitation occurs when microbubbles in the liquid rapidly collapse inducing a shock wave. In sonochemistry, ultrasound is used as a processing aid to accelerate chemical reactions. Ultrasound produces high local temperatures, pressures and rapid temperature changes and thus it is widely used in materials chemistry [42].

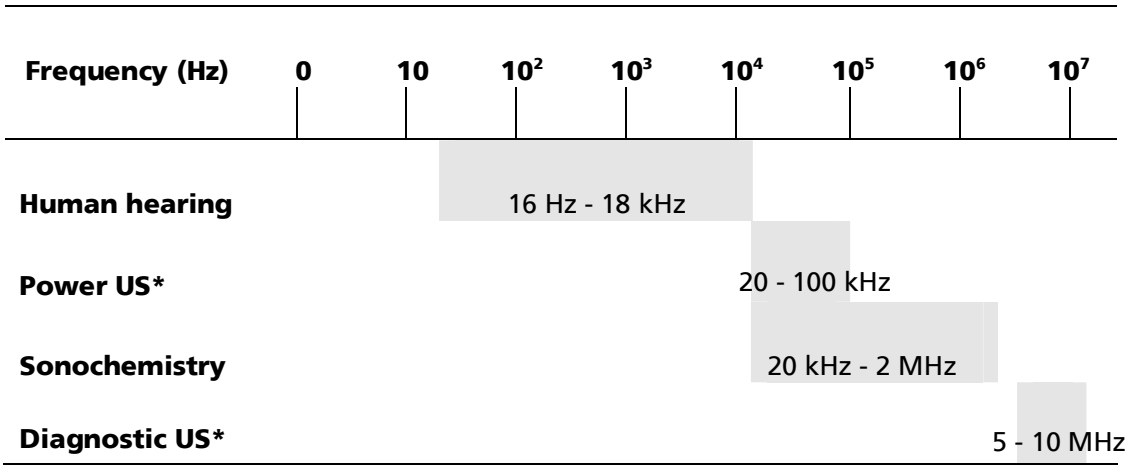

Figure 6 *Frequency (Hz) ranges of sound. *US, ultrasound. Modified from Mason (1999) [161].*

2.6.2 Possibilities for ultrasound processing

Ultrasound offers versatile possibilities as a processing aid for different kinds of industries [162]. From the pharmaceutical point of view, the most interesting processing applications are the fluidisation of powders and granular materials, decrease of friction between particles and die walls, handling of living cells, crystallisation, impact grinding, extrusion and diffusion, agglomeration in suspensions, the treatment of fibers, cleaning and homogenisation. Thus far, ultrasound has been used in pharmaceutical technological processes such as crystallisation [43], tableting [163], granulation [164], diagnostics and cleaning.

The six most frequent applications of ultrasound are cleaning, plastic or metal welding, extraction, homogenising, atomisation and machining [158]. Plastic remains solid in ultrasonic cold forming/welding, probably due to the reduced internal friction [162]. Ultrasound is widely used in food processing to increase mass transfer in gas-solid and liquid-solid masses [165] (Table 3). The flow properties of highly viscous and sticky materials in metal tubes can be improved by ultrasonic treatment [166]. In the food industry, solutions of this kind have been used in production of sausages, for instance. In addition, ultrasound-assisted welding is used in the sintering of cylinders and capsules [167].

High-intensity ultrasonic devices are used in sonochemistry to modify material surfaces and properties and to produce amorphous materials [42]. Ultrasound has also been used in the crystallisation of materials since the beginning of the 70's [168]. In addition, ultrasound is used in laboratory-scale textile dying and in melt mixing [169,170]. Dye penetration into fibers can occur only at temperatures above T_g. It has been reported that ultrasound does not change the T_g of amorphous materials [171]. It can also be used as flow enhancer in porous media during filtering and in impregnation.

Ultrasound is found to increase paper wetting, because it releases air bubbles and thus it increased capillary wetting [172]. Wetting is probably increased in materials that are thick or have a tortuous pore structure. Similarly, the penetration of liquids into materials with moderate or high contact angles is increased. In addition, ultrasound increases sorption and diffusion of liquid into/onto material [173,174]. Ultrasound may also transfer and dislocate wood fibres [175]. It changes interfaces between phases. Ultrasound is found to decrease the required operating temperature as well as viscosity and die pressure in the extrusion process [176]. It was also observed to increase the mass flow and to produce good appearance of extruded material.

Table 3. *Usages of ultrasound in food processing [177].*

Mechanical effects	Chemical and biological effects
Crystallisation	Bactericidal action
Degassing	Effluent treatment
Destruction of foams	Modification of growth of living cells
Extraction of flavourings	Alteration of enzyme activity
Filtration and drying	Oxidation
Freezing	Sterilization of equipment
Mixing and homogenization	
Precipitation of airborne powders	
Tenderization of meat	

2.6.3 Ultrasound cutting

Ultrasonic cutters were introduced in the food industry during the 1990s. There are several advantages to ultrasound cutting that explain the current popularity in the food industry (Table 4). The blades vibrate longitudinally at a frequency of approximately 20 kHz and the machines are fully automated [178]. Ultrasound cutters have been used for cutting difficult materials like soft cream cakes and sticky confectionary. A possible pitfall in ultrasound cutting is the heating of the ultrasound cutting blade [179] and possible chemical/physical changes in the cut of surfaces [180]. These changes are fortunately related to cutting time and power used. Furthermore, ultrasound cutting blades are more expensive than traditional blades, but it is estimated that the investment will pay itself back in one year [178]. In the literature usage of ultrasound cutting in the pharmaceutical industry has not been described.

Table 4. *Benefits of ultrasound cutting compared with a traditional cutting blade. Modified from Rawson (1998) [178].*

Quality of the cut face is visually excellent
The product is virtually undisturbed
Multi-layered products or hard particles contained in a soft matrix can be cut
Smearing is reduced
The required cutting force is significantly reduced
Multilayered products can be cut easily
The blade is self-cleaning
If cavitation is used, it kills bacteria
Crumbs and waste are significantly reduced
Brittle products have less tendency to break
It is cost effective, having low running costs
Less sharp blades are needed and longer intervals between sharpening than in conventional blades
Can be easily automated
Cutting speeds are similar to conventional methods

3. Aims of the study

The main aim of the present study was to develope a processing method for the formulation of a solid dosage form with 200 mg or more of an amorphous low molecular weight model substance in a single pharmaceutical unit form. The model substance had a low T_g (below 20 °C) and thus the formulated materials were sticky in ambient conditions. The diameter of the dosage form should be less than 9 mm. The formulating method should be quite economical and simple. The specific aims were:

1. To find a cheap and physically stable amorphous model material for large scale processing studies that could be used in formulation tests instead of the actual drug substance of interest, which is sticky, amorphous, highly potent and expensive;

2. To characterise the physical/chemical properties of this model material;

3. To develop and compare physical testing methods for amorphous materials and amorphous binary mixtures;

4. To study prerequisites for good physical stability against crystallisation in amorphous binary mixtures by different analytical methods;

5. To develop a processing method for amorphous materials with a low glass transition temperature;

6. To gather information for how to measure stickiness and how to avoid it during processing.

4. Experimental

4.1 Materials

The model materials used were citric acid anhydrate (CAA) (USP) and monoclinic paracetamol (PARA) (USP), which were purchased from Hawkins Inc. (Hawkins Inc., MN, USA) (I-V). Some physical properties of these materials are shown in Table 5.

Table 5. *Physical properties of citric acid anhydrate and paracetamol. Modified from papers I and V.*

Physical property	Citric acid anhydrate	Monoclinic paracetamol
Molecular structure [a]	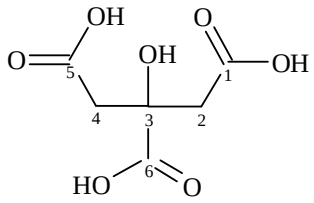	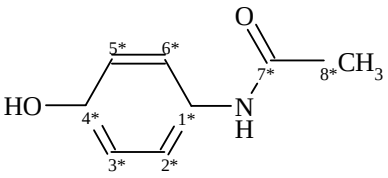
Molecular weight	192.1 g/mol	151.2 g/mol
Melting point	153 °C	169 °C
pKa	3.1; 4.8; 6.4	9.4
Glass transition (onset)	11 °C	22.3 °C
Water solubility at 22 °C	10 g/100 ml	0.1-0.5 g/100 ml
Hydrogen bond acceptors	$-OH_{alc}$, $-OH_{ac}$, C=O	-OH, C=O
Hydrogen bond donors	$-OH_{alc}$, $-OH_{ac}$	-OH, NH

[a] Atom numbering as in article V.

4.2 Processing methods

4.2.1 Sample preparation of binary mixtures (I, II, III, IV, V)

Melting was selected as the most suitable method for producing the amorphous material (I, II, III, IV, V). The melting method is widely used in pharmaceutical research. However, an ethanol evaporation method was also tested as a reference to produce amorphous material at a lower processing temperature than that used in the melting method (II).

Melt-quenching of bulk materials (I, II)

An electric heating furnace equipped with a temperature controlling system was used to melt the various blends. Batch size was 50 g and the materials were added to the furnace at 100 °C. The sample was mixed by hand with a glass rod. The starting point for melting was defined as the time at which the sample achieved the target temperature, shown in Table 6. The melt was poured onto two aluminium pans floating on liquid nitrogen and cooled to the final temperature of 20 °C ± 10 °C.

Table 6. *Experimental design to prepare the most suitable/physically stable melt-quenched material for processing studies. Modified from paper I.*

Composition	Melting time 2 min			Melting time 6 min			Melting time 10 min		
PARA % (w/w)	172 °C	179 °C	186 °C	172 °C	179 °C	186 °C	172 °C	179 °C	186 °C
0	x,o		x		x		x		x
25		x,o		x		x		x	
50	x		x		x,o		x		x
75		x		x,o		x		x	
100	x		x		x		x		x,o

x, test and o, duplicate.

Ethanol evaporation (II)

The ethanol-evaporated materials were pure citric acid, 25/75 and 50/50 (paracetamol/citric acid anhydrate, %, w/w). The sample size used was 6.0 g of dry materials. The materials were dissolved in 15 g of 96% (V/V) ethanol (Altia, Rajamäki, Finland). The solution was poured into an aluminum pan on a thermostatted hot plate (110 °C ± 10 °C) with a vacuum chamber (100 mbar). The samples were held under these conditions until the residual weight was from approximately 4% to 10% w/w, after which they were placed in a vacuum oven (110 °C, 40 mbar). The samples were held in the oven as long as the residual weight was less than 0.5% (w/w) of the total weight of added dry powder.

Ultrasound processing (III, IV)

The batch size was 100 g and the composition was 50/50 blend (w/w, %). Melting time was 6 min at 179 °C ± 2 °C in the heating furnace. The hot melt was poured into a cylinder (Ø 30 mm) coated with Teflon and the sample was cooled to room temperature.

Melt blending (V)

PARA and CAA were melted in separate glass beakers after which materials were mixed and poured onto an aluminium plate. Melting temperatures

were 163 °C and 179 °C for CAA and PARA respectively. Batch size used was 2 g. The blends contained 25%, 50% or 75% of paracetamol (w/w).

4.2.2 Ultrasound extrusion and cutting (III)

For ultrasound cutting and extrusion, the input of ultrasonic power was adjusted using an ENI Model 1104LA amplifier and the frequency was set using an Aitrel/American Reliance Inc. function generator Model FG-506. Langevin-type piezoceramic sandwich transducers were used in both the knife and nozzle.

Ultrasound-assisted extrusion
The ultrasound nozzle was constructed to give the maximum ultrasound amplitude in the longitudinal direction (Figure 7). The nozzle system was insulated from the sample tank with a hydraulic pipe to maintain a constant working frequency in the ultrasound nozzle (18.77 kHz). The piston was driven by pressurized air with a constant pressure of 5.4 bar. The ultrasound pulse during mass flow was 60 s ± 5 s. The variability was due to nozzle warming-up during the ultrasound pulse. With the help of ultrasound pulsing, the effect of warming-up of the nozzle on mass flow could be evaluated. Pulses used during the experiment varied from 3 to 5. Extrudate was forced through a 3 mm diameter orifice and extrudates were collected on a moving paper (extrudates were kept separate) or on an aluminium pan (extrudates were in contact with each other). The factors in the design of the experiment were the ultrasound power in the nozzle and temperature of the material in the sample tank and in the ultrasound nozzle (Table 7).

Table 7. *Design of the experiments on ultrasound-assisted (A) extrusion and (B) cutting. Modified from paper III.*

(A)

Power [W]/ Temp. [°C]	0 W	50 W	100 W	150 W
50	x,o	x,o	x,o	x
60	x,o	x,o	x,o	x
70	x,o	x,o	x,o	-*

(B)

Power [W]/ Temp. [°C]	0 W	50 W	100 W
25	x	x	x
40	x	x	x
50	x	x	x
60	x	x	x

x, test, o, duplicate.
*Not measured due to rapid mass flow.

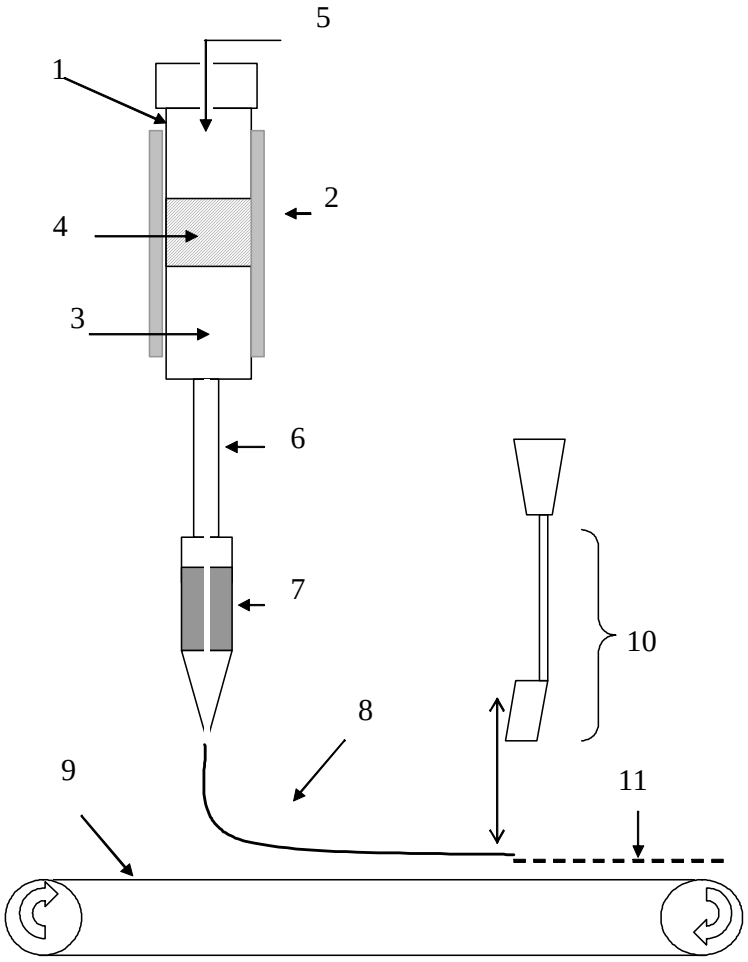

Figure 7 *Schematic cross-sectional representation of the ultrasound equipment used in the ultrasound extrusion and cutting experiments. Description of equipment: 1, pre-melting chamber, 2, heating block, 3, sample, 4, piston driven by 5, pressurised air, 6, hydraulic pipe, 7, ultrasound nozzle with four piezoceramic sandwiches, 8, extruded material, 9, moving paper, 10, ultrasonic cutting knife, 11, cut extrudates. Modified from the patent application Hoppu (2007) [181].*

Ultrasound-assisted cutting

Materials used in the ultrasound-cutting test were extruded at 50 °C without ultrasound power in the nozzle. Extrudate was collected on a paper sheet. After extrusion, the extrudate was warmed up to 25 °C, 40 °C, 50 °C, or 60 °C with warm air (Table 7). After heating the ultrasound knife, working at a frequency of 24.89 kHz, was used to cut the extrudate into pieces. Ultrasound power levels used in the knife were 0 W, 50 W or 100 W. The knife was air-cooled during the cutting process.

4.3 Analytical methods

4.3.1 High-performance liquid chromatography (I, II, IV, V)

The chemical purity of materials was confirmed using an HPLC (Thermo Separation Products, San Jose, CA, USA) equipped with an UV-VIS detector (model FOCUS, San Jose, CA, USA). Wavelengths used for detection were 215 nm for CAA and 245 nm for PARA. The eluent used was composed of 96% (V/V) water with 0.1% (V/V) trifluoroacetic acid at pH 2.1 and 4% (V/V) acetonitril. The injection size was 10 µl and the flow rate was 1 ml/min in an RP-18 column (150 x 4.6 mm, 5 µm, Supelco, Bellafonte, PA, USA).

4.3.2 Water content analysis (I, II, IV, V)

The amount of water in the samples was measured with a Karl Fischer titrimetry (Mettler-Toledo AG, model: DI35, Greifensee, Switzerland). Hydranal® solvent (Riedel de Haën, Seelze, Germany) was used as a volumetric solvent and Hydranal® titrant 5 as a volumetric titrant.

4.3.3 Raman scattering (I)

Control Development Raman spectrometer (Control Development Inc., South Bend, IN, USA) was used to acquire the spectra from 170 cm^{-1} to 2200 cm^{-1}. The spectrometer was equipped with a thermoelectrically cooled CCD detector and a fibre optic probe (RamanProbe, InPhotonics, Norwood, MA, USA). The power of the laser source was 500 mW at 785 nm (Starbright 785S, Torsana Laser Technologies, Skodsborg, Denmark). The rotating sample holder was rotated at approximately 30 rpm during the measurements. The integration time was 3 s and the median spectrum of three spectra was constructed based on baseline and standard normal variate (SNV) transformation [182].

4.3.4 Fourier transform infrared microscopy (I, II, IV)

Fourier transform infrared microscopy (FT-IR) spectra were acquired over a spectral range of 650 cm^{-1} to 7500 cm^{-1} with a Hyperion 1000 microscope (Bruker Optik GmbH, Ettlingen, Germany). The microscope was used to identify polymorphs of crystals formed on the material surface. Specular reflectance spectra were averaged from 64 scans at a resolution of 4 cm^{-1}. The Kramers-Kronig transformation was carried out using the software package provided (Opus 5.1, Bruker Optik GmbH, Ettlingen, Germany).

4.3.5 Thermal analysis (I, II, IV, V)

The *glass transition temperature (T_g)* of the bulk samples was measured with a Mettler TA 4000 DSC instrumented with a DSC-30 low temperature cell (Mettler-Toledo AG, Greifensee, Switzerland) (I). Both onset (extrapolated) and midpoint values were determined for T_g. Two scans were made for each sample over the same temperature range from 60 °C to 100 °C. The heating rate was 10 °C/min and the programmed cooling was used (I).

The *in situ* melting was carried out by heating the samples in the DSC to 170 °C, 175 °C and 180 °C, after which instant cooling was performed (I). Furthermore, *in situ* melting was also done at 179 °C for 6 min. The heating rate was 10 °C/min. Blends were made in a mortar and pestle before melting. Samples were prepared with and without a pinhole. The glass transition was scanned once from -40 °C to +50 °C (I).

Glass transition temperature, heating rate dependence, the specific heat capacity and physical stability of the material were measured using a Mettler-Toledo 823^e DSC (Mettler-Toledo AG, Greifensee, Switzerland) with a Julabo FT900 intercooler (Seelbach, Germany) with a pinhole in the sample pan (II, IV, V).

In the glass transition measurements, the temperature in the first scan ranged from -40 °C to 100 °C. The second scan was done from -40 °C to 150 °C (II, IV, V).

Enthalpic relaxation was measured using hermetically sealed pans. Pure PARA and CAA samples were melted *in situ* (chemical purity was more than 98% measured using HPLC). The temperature was 5 °C higher than the melting temperature and the melting time was 5 min, after which the samples were cooled to -40 °C at a cooling rate of 10 °C/min. Other samples used were 50/50 ethanol-produced and 50/50 melt-produced bulk samples. After cooling to -40 °C the samples were heated to 40 °C and cooled again to destroy the thermal history. The sample was heated from -40 °C to the storage temperature and held there for a specific time. The annealing times were 1, 2, 3, 4, 8, 16, and 24 h, after which the material was cooled again to -40 °C. The sample was scanned twice from -40 °C to 40 °C to measure enthalpy recovery in the first scan (ΔH) and to measure the total enthalpy recovery in the second scan. Heating and cooling rates were 10 °C/min and annealing temperatures were 10 or 20 °C lower than T_g (accuracy ±1 °C).

Heating rate dependence was used to charaterise fragility parameters (D and T_0) using the normal DSC mode. Measurements were made as described by other researchers [93] except that samples were cooled to a temperature at 40 °C (not 50 °C) lower than the T_g. T_g midpoints were used to define fragility and activation enthalpies. Heating and cooling rates were: 2, 5, 10, 15, and 20 °C/min.

The specific heat capacity (C_p) was measured using a MDSC from Mettler-Toledo (TOPEM). The thermal history of samples was destroyed, as in the enthalpic relaxation measurements. Samples were scanned at a temperature range of -20 to 40 °C with a heating rate of 1 °C/min, amplitude 0.5 °C and

frequency variation of 15 to 30 s. The C_p of crystalline blends were measured from crystalline starting materials weighed directly in the DSC pan in the right ratio.

4.3.6 X-ray powder diffraction (I, II, IV)

An X-ray powder diffractometer (XRPD) was used to study the solid state of the materials and to identify polymorphs in the partly crystalline/crystalline materials (Bruker AXS D8 advance, Bruker AXS GmbH, Karlsruhe, Germany). The XRPD was operated at 40 kV and 40 mA using CuKα radiation. The diffraction angle varied from 10° to 40° (2θ) with steps of 0.1° per 2 sec. The reference codes used to identify polymorphs were HXACAN07 for monoclinic, and HXACAN08 for orthorhombic PARA [183], and CITRAC10 for CAA, and CITARC for citric acid monohydrate [184,185] (CSD, The Cambridge Crystallographic Data Centre, Cambridge, UK).

4.3.7 Resistance to deformation and stickiness (III)

Resistance to deformation and stickiness were tested using a LLOYD material tester (Lloyd LRX, Lloyd instruments Ltd., Fareham Hampshire, Great Britain) combined with a specially designed sample compartment (Figure 8). The purpose of the test was to measure material deformability in compression and to test the stickiness of the material in decompression. The materials measured are those listed in Table 6. Melt samples were poured into a four/five hexagonal nut (Ø 10mm, 7 mm deep), used as a sample holder in the LLOYD material tester. The nut was screwed into a sample holder, which was covered with a transparent sample compartment. Heated air was used to control the temperature in the sample compartment. Measurement temperatures were 25 °C, 30 °C, 35 °C, 40 °C and 45 °C. The diameter of the flat steel punch was 5 mm. The steel punch was pushed into the sample 5 mm and after that pulled off. If a load limit of 90 N was achieved in the compression, the punch was automatically pulled off from the sample. Preload in contact was 0.5 N and the driving speed of the punch was 3 mm/min in decompression and compression. The resistance to deformation was evaluated from the compression curve by calculating the slope (N/mm). The stickiness was determined from the minimum force (N) in the decompression curve.

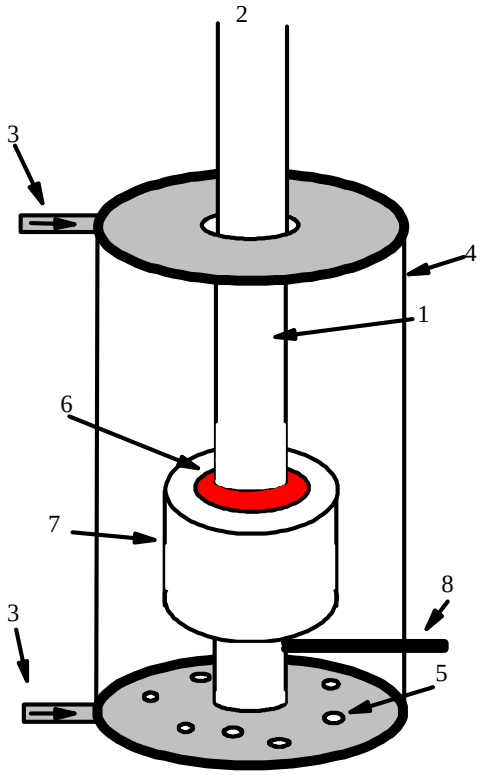

Figure 8 *Schematic representation of the apparatus used to study stickiness and resistance to deformation: 1, a steel punch driven by 2, the LLOYD material tester, 3, heating gas flowing inside the sample compartment 4 through the holes in the bottom 5 or roof, and 6, material in the sample holder 7 equipped with a thermometer 8.*

4.3.8 Rheology (II)

Rheological measurements were made from selected melt-produced samples. Measurements were carried out using a TA Instruments AR2000 controlled stress rheometer (TA instruments, DE, USA). For dynamic measurements, the linear region was established by performing a strain sweep, while frequency sweeps were made typically in the frequency range of 0.01-100 rad/s. In steady shear flow measurements, shear rates from 0.1 to 500 1/s were applied in a controlled rate mode.

4.3.9 Solid state nuclear magnetic resonance (V)

The physical stability of the physical mixtures and amorphous blends were studied measuring, 1, normal solid-state ^{13}C NMR spectra (result: molecular interactions from the ^{13}C chemical shifts), 2, rotating-frame spin-lattice relaxation for protons ($T_{1\rho}$) (result: homogeneity of blends), and 3, variable

temperature measurement (results: molecular mobility and dynamics of the blend) (Fig. 9). Experiments were done using a Bruker 400 MHz spectrometer with a wide bore magnet, equipped with a double resonance CPMAS probe (Bruker Analytik GmbH, Rheinstetten, Germany). The milled samples were inserted into the Bruker 4 mm rotors (zirconium dioxide rotor with the Kel-F® endcap). A boron nitride endcap was used in variable temperature measurements.

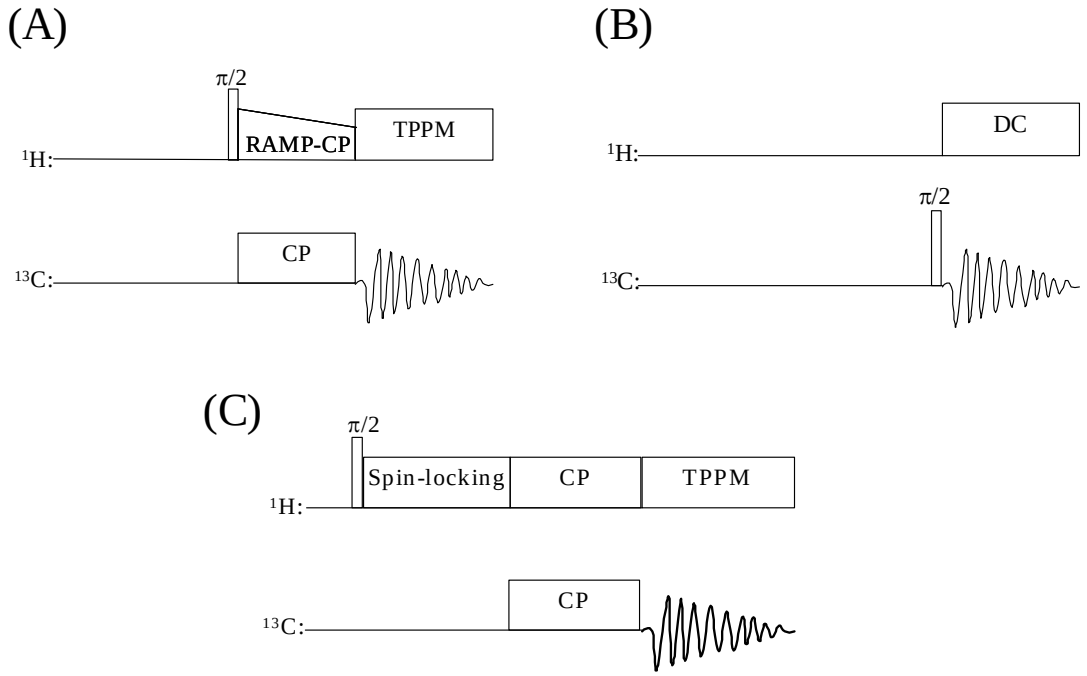

Figure 9 *Pulse sequences for (A) CP/MAS ^{13}C 1D spectra, (B) measurement of temperature dependence for the spectral line width and (C) measurement of proton rotating-frame spin-lattice ($T_{1\rho}$) relaxation. CP, cross-polarisation, RAMP, ramped mode, DC, proton decoupling, TPPM, two pulse phase modulation.*

4.3.10 Optical and stereo microscopy (IV)

Polarizing light microscopy (DAS Mikroskop Leica Microscopie und Systeme GmbH, Wetzlar, Germany) was used to study birefringence and the amount of crystals in the extrudates. An optical stereomicroscope (Leica MZ6, Leica Mikroskopie und System GmbH, Bensheim, Germany) was used to compare the appearance of differently prepared extrudates.

4.3.11 Aging study (I, II, IV)

After sample preparation (bulk and ethanol evaporated materials) aluminium pans were placed in silica desiccators with a relative humidity (RH) of approx. 3% to stabilise for 12 hours (I, II). Samples were then characterised by HPLC, FT-IR, XRPD, Karl Fischer titration, DSC, and Raman scattering. After this initial characterisation, one sample pan was exposed to 43% RH (desiccator containing K_2CO_3 solution) and the other pan was placed in a desiccator over a dry silica desiccant. Samples in 43% RH were analysed at 1, 4, 8, 12, and 18 weeks after melting, whereas the dry samples were analysed after 9, 18, 27, 52 and 104 weeks with FT-IR, XRPD, Karl Fischer titration, and Raman spectroscopy.

Ultrasound treated materials were characterised after 1, 4, 8, 16, 26 and 52 weeks of storage over silica desiccant (IV). Samples used in the enthalpic relaxation study (II) were stored in dry conditions at -20 °C for one year after which they were measured with DSC to check their physical stability.

4.3.12 Statistical methods (I, II, III, IV, V)

The design of the experiments and data analysis were made by the Modde programme version 7.0 (Umetrics AB, Umeå, Sweden). Spectral and DSC data were evaluated with multivariate data analysis using Simca-P version 10.5 (Umetrics AB, Umeå, Sweden). The designs of the experiments were based on the full factorial interaction models described in papers I, III and IV. In DSC thermograms, Raman and FT-IR spectra, the median of thermograms/spectra was selected and shown in the figures.

5. Results and discussion

More detailed results and discussions can be found in the respective papers (I-V). A schematic approach used in the present study the physically stable amorphous binary mixtures with low glass transition temperatures and other process materials of this kind is shown in Figure 10.

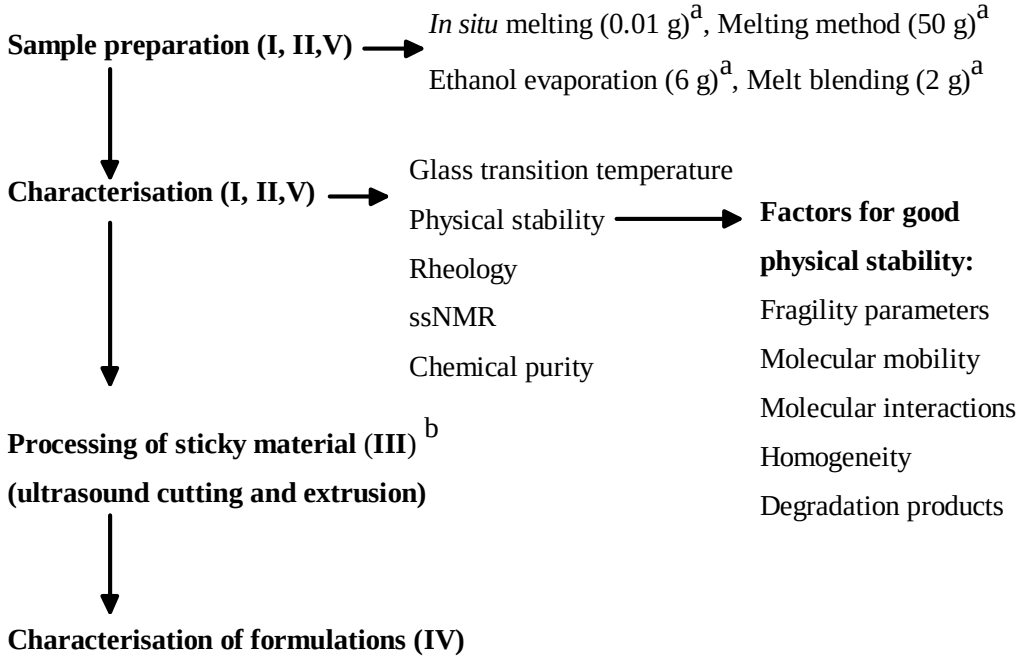

Figure 10 *A schematic description of the study plan used in this study. [(a)] Batch size, [(b)] melting method using a batch size of 100 g.*

5.1 Effect of composition and sample preparation method on amorphous binary mixtures

5.1.1 Glass transition temperature (I, II, IV, V)

In all the differently prepared materials, T_g was observed to increase as the ratio of PARA increased (Figs. 11 and 12). The T_g of materials prepared by the melt blending method, was found to be higher than in materials with the same composition but prepared by other production methods. This was due to a smaller amount of degradation products formed in the melt-blended materials than in other materials (I, II, V). Batch size during melting of CAA has an effect on the amount of degradation products [186,187]. It is known that volatile degradation products are difficult to evaporate from citric acid

blends [188], possibly due to the high hydrogen bonding capacity of CAA and high viscosity of the melt.

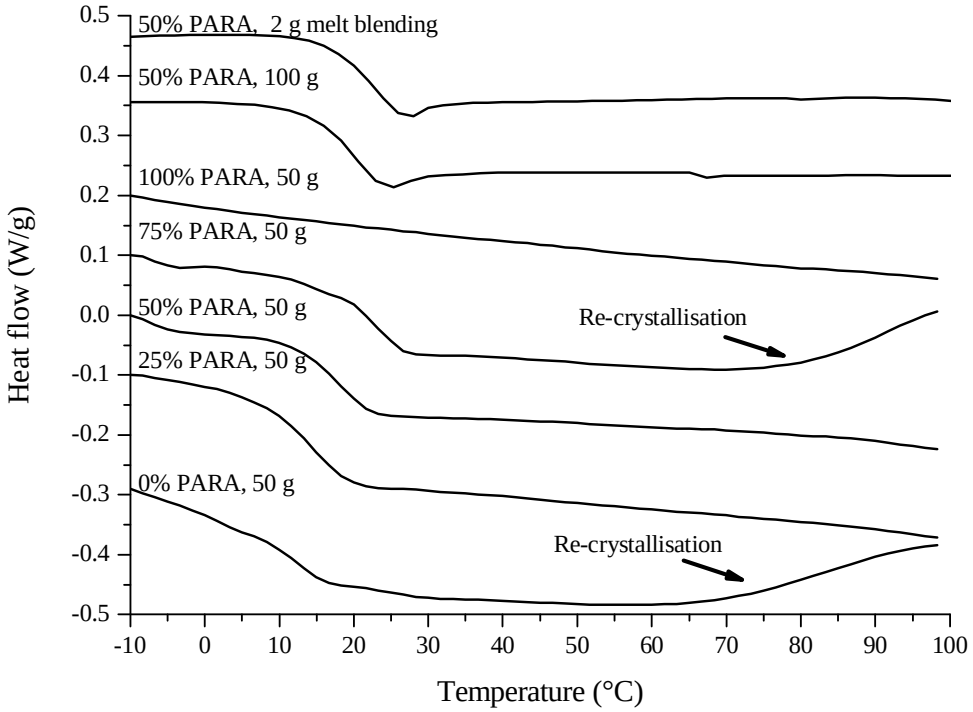

Figure 11 *Effect of batch size and amount of paracetamol (w/w, %) on glass transition temperature. Modified from papers I, IV and V.*

In melt-blended blends, the measured T_g's were higher than the one estimated from the simple additivity of T_g (calculated using Fox equation [189]) while in the bulk-prepared materials the blends had lower values. The positive deviation from the simple additivity of T_g has been reported previously [109]. The negative deviation from the simple additivity of T_g was related to the degradation products formed during sample preparation. Underestimation was observed especially in the *in situ* materials measured without a pinhole (I). For melt-blended materials, T_g^{mid} values were 16.3 °C and 19.3 °C, for 25% of PARA (w/w) and 50/50 blend, respectively. These T_g^{mid} values were slightly higher than observed for bulk-prepared blends with the same composition, where values for T_g^{mid} were 14.7 °C and 17.9 °C, respectively (I, II). For the ultrasound processed 50/50 reference material, T_g^{mid} was 15.3 ± 0.2 °C (III). Differences in T_g might be related to the higher melting temperature and longer melting time for bulk-prepared materials than for melt-blended materials. In all the blends, CAA was found to be more sensitive to degradation than PARA but it was also dependent on the composition (I, II).

The extreme melting conditions, coupled with the long exposure to heat and the high melting temperature, increased the degradation products in the

material as expected. The chemical purity of materials has an effect on T_g because degradation products may plasticise the material and thus purity has an effect on the T_g (I). The smaller amount of degradation products in melt-blended materials than in bulk-prepared materials was confirmed in HPLC analysis and it was also seen in ^{13}C NMR spectra, where no extra peaks were observed. This kind of melt blending method has also been described elsewhere in preparation of amorphous solid dispersions [190]. Thus, production scale and preparation method has an effect on the amount of degradation products formed and thus on the T_g.

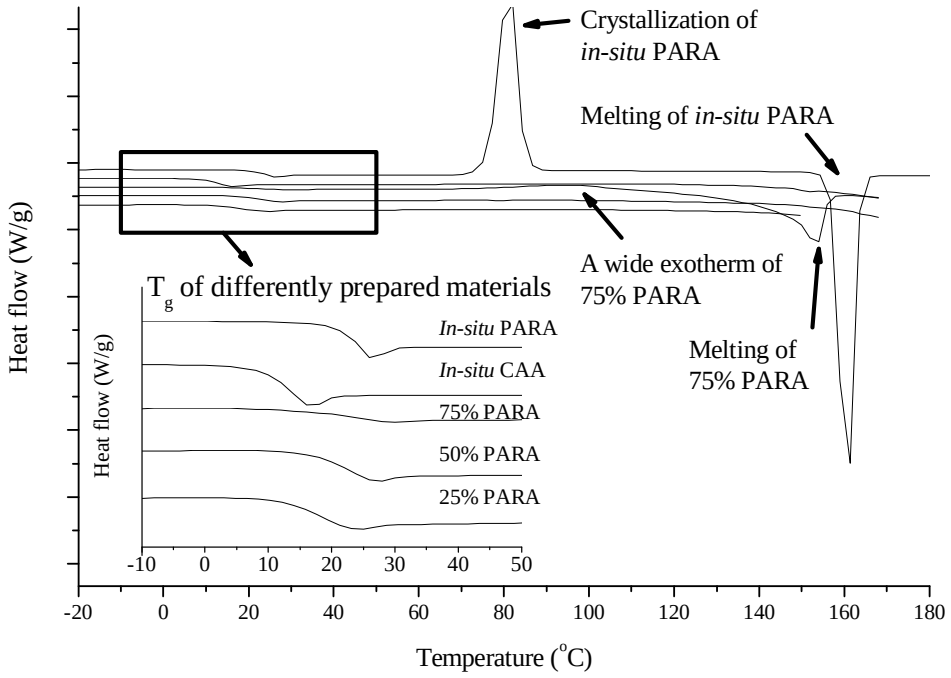

Figure 12 *Glass transition of melt-blended materials compared with the in situ prepared pure PARA and CAA. In the upper DSC thermograms, crystallisation of in situ PARA and melting endotherms of in situ PARA (orthorhombic form) and the blend containing 75% PARA (w/w) are also presented.*

5.1.2 Physical stability against crystallisation (I, II, IV, V)

The crystallisation of amorphous materials happened faster over 43% RH than over 3% RH (Table 8) (I). This was probably related to the fact that water plasticise the material. Water may also change molecular interactions in the material because water is a potent hydrogen bond-competitor. Changes in hydrogen bonding between molecules can induce crystallisation.

Crystallisation started on the surface of the amorphous material. This finding supports the key role of water in crystallisation because the surface has the best contact with the humid air. In addition, re-crystallisation re-

distributes the water in the partly crystalline material because an amorphous state holds more water than a crystalline state [191]. Redistribution of water plasticises the rest of amorphous matrix, which accelerates the crystallisation rate due to decreased viscosity (increased molecular mobility). Similar results have also been observed for e.g. indomethacin [192]. Furthermore, the water uptake of a crystalline biphasic system (citric acid anhydrate/sucrose) has been found to be higher than for the individual components [193]. This might also occur in our CAA/PARA mixtures where amorphous blends absorbed/adsorbed more water than, for example, pure partly amorphous CAA (I). The blends were observed to be physically more stable than the pure materials in the aging studies. The melting conditions were found to have a minimal effect on the overall crystallisation rate (I). PARA had a stronger tendency to crystallise from the blends than CAA when studied with FT-IR microscopy (II) and ssNMR (V).

In DSC studies (Figs. 11 and 12), it was found that materials containing a high amount of PARA or pure CAA crystallised more easily than other materials (I, II, V). Furthermore, storage time before measurement had an effect on the crystallisation during DSC scan. This was extremely well seen in the pure CAA that did not crystallise in *in situ* melting studies, but the bulk-prepared CAA crystallised easily during the DSC scan. This was related to the crystals formed in the materials that had been formed due to ineffective cooling or storage.

Table 8. *Physical stability of materials prepared by different methods. Letters stand for different samples with different batch size that were observed to crystallise during sample preparation, material measurement or aging: a) bulk 50 g, b) ethanol 6 g and c) melt blending 2 g. Modified from papers I, II, V.*

	Sample preparation		**Measurement**		**Aging at RH[(ii)]**			
w/w (%) PARA	*In situ*[(i)]	During preparation[(ii)]	DSC[(i)]	Rheometer[(ii)]	1 week at 43%	4 weeks at 43%	52 weeks at 3%	104 weeks at 3%[(iii)]
0	-	a	a	a	a, b	+	+	+
25	-	-	-	a	-	+	-	-
50	-	-	-	-	-	+	-	-
75	-	b	+	+	a, b	+	b	+
100	+	+	+	+	+	+	+	+

-, materials did not crystallise during preparation, measurement or aging.
+, all the materials crystallised regardless of preparation method
i, material crystallised during the first DSC scan
ii, physical stability measured by XRPD
iii, only 50 g bulk-prepared materials were measured

Consecutive shearing at different temperatures was found to be an extremely effective method to crystallise unstable blends and it was observed to correlate with the actual physical stability during long-term storage in dry conditions (Fig. 13) (II). In dry conditions, amorphous bulk-prepared blends (25/75 and 50/50) were found to still be amorphous after at least two years when measured by XRPD (II).

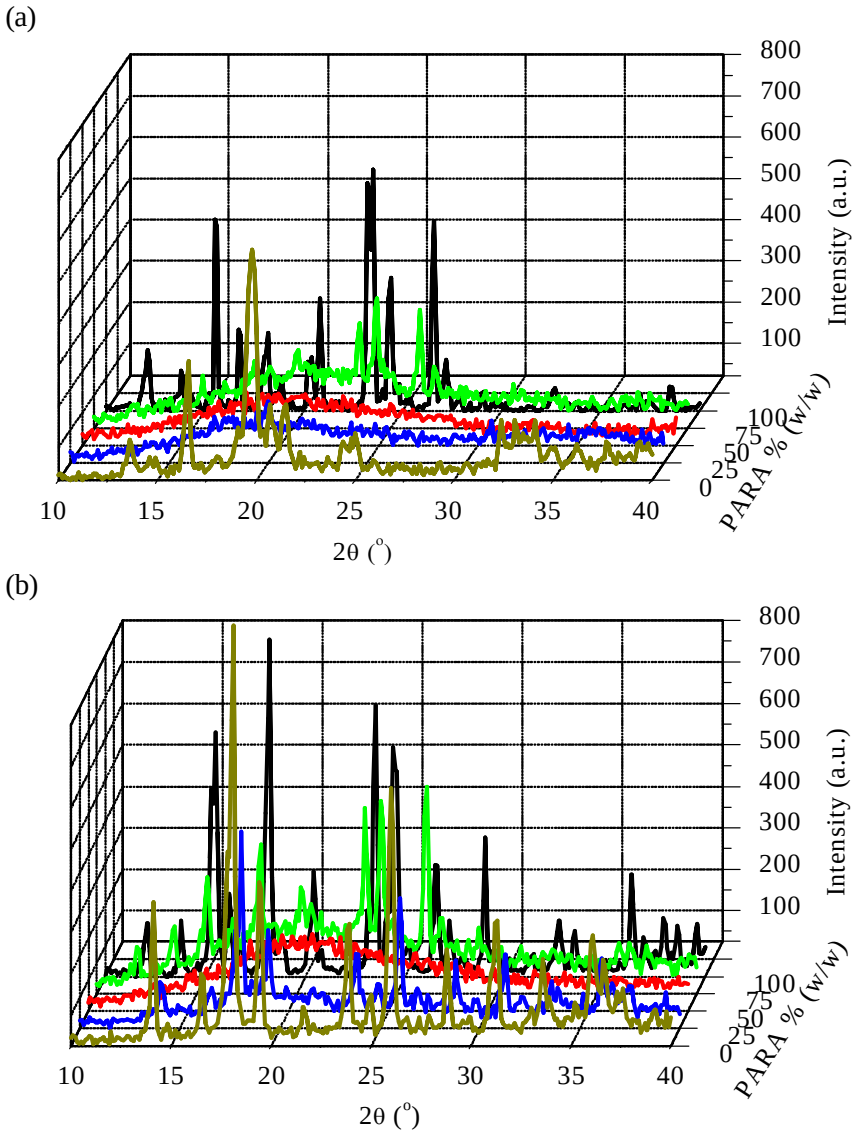

Figure 13 *XRPD analysis of melt-produced bulk materials (a) after two years storage over dry silica, (b) after consecutive shearing.*

The 50/50 (w/w, %) blend did not crystallise upon consecutive shearing regardless of the preparation method (II). Ethanol evaporated materials (physically stable from 0 to 50 wt-% PARA) and melt-blended materials (25 to

50 wt-% PARA) were observed to be more stable upon consecutive shearing than the 50 g bulk-prepared materials. This might be related to the more homogeneous blends of these materials resulting in a lack of formed crystals.

Karis and co-authors (1995) [194] reported shear-induced crystallization during viscosity measurement. Their explanation was the coupling between molecules with hydrogen bonds induced by external strain. Alignment is observed to form shorter hydrogen bonds that improve hydrogen bond stability against shearing [195]. CAA crystallises owing to the dimerisation of carboxylic acid groups of CAA (I). Dimerised carboxyl acid has particularly strong hydrogen bonds. After shearing, pure CAA had high intensities in XRPD diffractograms at 16.5° and 19.5°, which were connected to the dimerisation of CAA (I). Alignment under shear has also reported to form relatively strong van der Waals forces in fats [196]. Similarly, alignment of PARA molecules is needed to form unit cells of monoclinic PARA where relatively strong van der Waals forces are crucial. Thus, batch size and processing method have a huge impact on physical stability. The chemical stability of blend materials decreased approximately 5% from the initial level during two years storage in dry conditions.

5.1.3 Rheology (II, V)

Viscosity of materials as a function of temperature is shown in Fig. 14. Viscosity was observed to increase as the amount of PARA in the composition increased. It can be seen that ethanol evaporated materials had lower viscosity than melt-processed materials. Furthermore, the dynamic moduli (G' and G'') of melt-produced blends were found to be slightly higher than for ethanol evaporated materials (II). The viscosity of melt-blended materials was slightly higher than that of bulk-prepared materials, probably due to a small amount of degradation products or water in the materials. Generally, it was found that the degradation products of CAA and PARA had only a minor effect on viscosity when similarly prepared materials were compared. Viscosity was more dependent on the preparation method due to changes in the amount of degradation products formed. Water content of the 50/50 melt-blended material was approximately 0.7% (w/w) while in the bulk-prepared material it was approximately 1.2% (II, V). All the materials behaved as viscous Newtonian liquids. For all the materials measured, the extrapolated viscosity at the T_g^{mid} lower than the often quoted 10^{12} Pa·s for glassy materials [56].

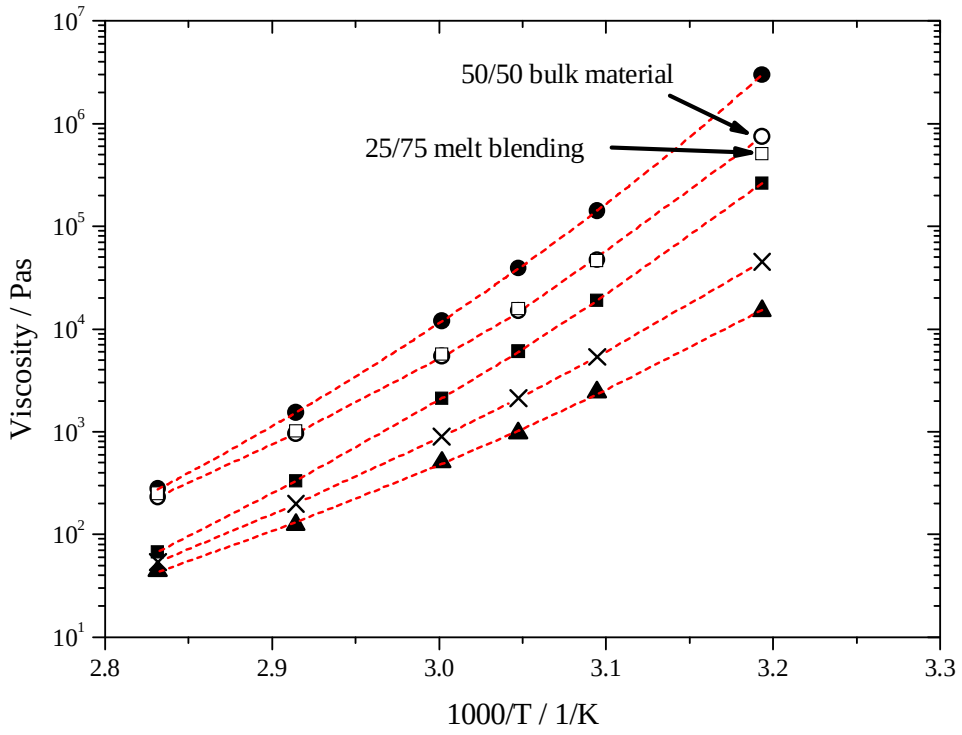

Figure 14 *Reciprocal temperature plot of viscosity of: ethanol-evaporated materials, citric acid (▲), 25 wt% (x), 50 wt% (■) PARA/CAA mixture; and melt-processed 50 wt% (o) bulk material, and melt-blended 25 wt% (□), 50 wt% (●) PARA/CAA mixture. Dashed lines are fit of VTF equation to the data between 40-80 °C. Modified from papers II and V.*

Due to the limited torque range of the rheometer, only data at low shear rates could be measured at 40 °C and 50 °C. In steady shear flow measurements, when higher shear rates were applied, the materials exhibited noticeable shear thinning, which probably resulted from slipping of the rheometer plate, especially as shear thinning was not observed in the oscillatory data up to 100 rad/s. Several possible sources of experimental error in rheological measurements have been reported [196,197]. Poor contact between the plate and material produces different velocities for the sample and the plate. Usually, small molecules are locked within surface irregularities, but for molecules larger than the irregularities, slippage may occur [196,198]. Slippage can be avoided by using different widths of plates or by using roughened or ribbed plate surfaces [197,198]. In this study, only one plate size with a normal steel surface could be used, which might have produced the slippage.

5.2 Factors affecting physical stability of amorphous binary mixtures

The 50/50 (%, w/w) blend was observed to be physically the most stable system regardless of the preparation method (Table 8). The 50/50 mixture did not crystallise as easily under dry conditions or upon consecutive shearing as the other compositions. The reasons for this behaviour are discussed below.

5.2.1 Fragility parameters (II, V)

Composition and preparation and measurement methods were found to have an effect on fragility parameters (II). Pure materials had lower fragility parameters than the blends when similar measurement settings were used. Materials with a high D value formed glass more easily than materials with a low D value [80]. However, small changes in the viscosity had a huge effect on observed D and T_0 values. In Fig. 14, the D value is 6.6 for the 50/50 bulk and 11.8 for 25% (w/w) melt-blended material, although the viscosity curves were quite similar. Similarly, T_0 values were 241.9 K and 218.8 K, respectively.

Furthermore, fragility parameters reported in the literature vary considerably even when similar thermal methods are used. For example, D values reported for paracetamol range from 4.9 to 9.3 and T_0 from 240.5 K to 260.3 K [118,199]. Similarly, the fragility values for citric acid vary from 5.6 to 15.0 and T_0 from 200.7 K to 249 K [93,98]. In addition, calculated D and T_0 values usually vary between different measurement methods [200] because different methods probe different modes of molecular motion. Water content in the material has also effect on fragility parameters defined probably due to changes in molecular interactions [201]. Differences in the defined parameters used in the molecular relaxation equations might have a huge effect on evaluated τ [93].

5.2.2 Molecular mobility (II, V)

Because molecular mobility in the blends was fast (τ<100 s), it did not explain the good physical stability of the 50/50 blend against crystallisation at ambient temperature (II,V). All the materials were stable at least one year in dry conditions at -20 °C as expected from the molecular relaxation times evaluated (II). At temperatures below the T_g, molecular mobility was observed to be slow and molecular relaxation times were observed to lengthen during the annealing time (II). Although different fragility parameters were used, it was observed that the molecular relaxation time of the 50/50 blend was lower than the τ of the pure materials at temperatures below T_g (II). Molecular relaxation times τ^{KWW} and τ^0 were higher for pure PARA than for the blends (Table 9) (τ^{KWW} is not shown, because the differences in the β values

does comparisons between materials difficult). This differed from the actual physical stability at temperatures above T_g (II).

Although CAA/PARA blends (25% PARA and 50% PARA, w/w, 50 g materials) were supercooled melts at approximately 25 °C, they were still amorphous according to XRPD after two years of storage in dry conditions, even though τ was less than 100 s (II) (Tables 9 and 10). Thus, there must be factors other than the molecular mobility that stabilise the amorphous state. Other molecules have also been found to be physically stable in the supercooled liquid state, such as o-terphenyl (T_g = 245 K), which has been reported to be physically stable at ambient conditions for many years [51]. Molecular mobility estimated above T_g correlated well with the viscosity data (II). Similarly, τ evaluated from the viscometer data correlated well with the actual physical stability of the materials. Possible reasons for the good physical stability of these materials are high viscosity and a τ just above the solidification point after melt quenching, as proposed by White and Cakebread (1984) [56].

Table 9. *Rheometrically and calorimetrically determined values for τ, T_g^{mid}, D, T_0 and γ of amorphous materials used.*

Material/ parameter	T_g^{mid} [K]	D	T_0 [K]	γ [c]	τ^0 at 253 K [e] [days]	τ at 298 K [f] [s]	τ at 323 K [f] [s]
[c] PARA	293.9	9.9	231.4	0.86	13.3	8.04	$7.0 \cdot 10^{-4}$
[c] CAA	284.9	11.8	215.9	0.90	0.7	0.28	$2.1 \cdot 10^{-4}$
[c] 50/50 melt [a]	287.3	14.9	204.5	0.91	0.6	1.35	$1.4 \cdot 10^{-3}$
[c] 50/50 melt [b]	292.5	18.5	194.6	0.89	1.4	13.29	$1.5 \cdot 10^{-2}$
[d] 50/50 melt [a]	287.3	6.6	241.9	0.91	0.6	0.02	$3.4 \cdot 10^{-6}$
[d] 50/50 melt [b]	292.5	11.1	227.1	0.89	2.4	24.60	$2.4 \cdot 10^{-3}$

[a] Bulk samples, batch size 50 g
[b] Melt blending, batch size 2 g
[c] Calorimetrically determined
[d] Rheometrically determined
[e] Calculated by Eq. 5 (initial relaxation time)
[f] Calculated by Eq. 6 (VTF)

The average correlation time for molecular mobility obtained from the spectral line width measurements with ssNMR correlated better with the τ derived from a rheometer than with τ derived from a DSC data (V) (Table 10). In the ssNMR study, the maximum spectral linewidth was observed at approximately 325 K, corresponding to an average correlation time for molecular mobility of $2.0 \cdot 10^{-5}$ s to $1.9 \cdot 10^{-6}$ s. Decoupling field was observed to be the dominating interaction giving an average correlation time $<\tau>$ of $1.9 \cdot 10^{-6}$ s (V). Small changes in the measured water content and T_g of the material might have altered the viscosity observed, having an effect on

evaluated molecular relaxation times. Furthermore, it is well known that different measurement methods probe slightly different molecular mobilities and there is some uncertainty in measured results especially when fragility parameters are used.

Table 10. *Effect of measurement temperature, batch size and measurement method on the molecular relaxation times (τ) observed for the amorphous 50/50 blend measured by DSC and rheometer. Fragility parameters used in the calculations (Eq. 6, VTF) are shown in Table 9. Modified from papers II and IV.*

Molecular relaxation time (τ)				
	50/50 Bulk material		50/50 Melt blending	
Temp. [K]	DSC [s]	Rheometer [s]	DSC [s]	Rheometer [s]
295	4.0	0.10	$3.8 \cdot 10^{1}$	$1.1 \cdot 10^{2}$
305	0.14	$8.9 \cdot 10^{-4}$	1.5	1.0
315	$9.1 \cdot 10^{-3}$	$2.9 \cdot 10^{-5}$	$9.8 \cdot 10^{-2}$	$2.6 \cdot 10^{-2}$
325	$9.3 \cdot 10^{-4}$	$2.1 \cdot 10^{-6}$	$9.9 \cdot 10^{-3}$	$1.4 \cdot 10^{-3}$
335	$1.3 \cdot 10^{-4}$	$2.7 \cdot 10^{-7}$	$1.4 \cdot 10^{-3}$	$1.3 \cdot 10^{-4}$
345	$2.6 \cdot 10^{-5}$	$5.1 \cdot 10^{-8}$	$2.5 \cdot 10^{-4}$	$1.8 \cdot 10^{-5}$
355	$6.1 \cdot 10^{-6}$	$1.3 \cdot 10^{-8}$	$5.7 \cdot 10^{-5}$	$3.5 \cdot 10^{-6}$

5.2.3 Molecular interactions (I, II, V)

Molecular interactions were studied using ssNMR, FT-IR microscopy, Raman scattering and XRPD. Different spectroscopic methods confirmed detectable changes in amorphous and crystalline forms of CAA/PARA blends. Bands observed using FT-IR microscopy, ssNMR, and Raman spectroscopy were merged together in some spectral regions in the amorphous state. This was due to more mixed molecular interactions in the blends than in the crystalline pure substances. In particular, a lack of dimerised carboxylic acid groups of CAA in the amorphous blends was observed (I, V) (Fig. 15). In addition, peak shift variation in ssNMR and FT-IR spectra resulted from changes in the molecular interactions. These were especially seen in ssNMR spectra where alcoholic groups of CAA and PARA moved higher frequencies, describing probably stronger hydrogen bonds in the amorphous state than in the crystalline state (V) (Fig. 15). A low frequency shift of amide (CNH, peak 1* in Table 5) of PARA might be the result of extremely weak hydrogen bonding in the blend and the apparent low frequency shift of the carboxylic acid of CAA could be due to the loss of dimerisation of the carboxylic acid.

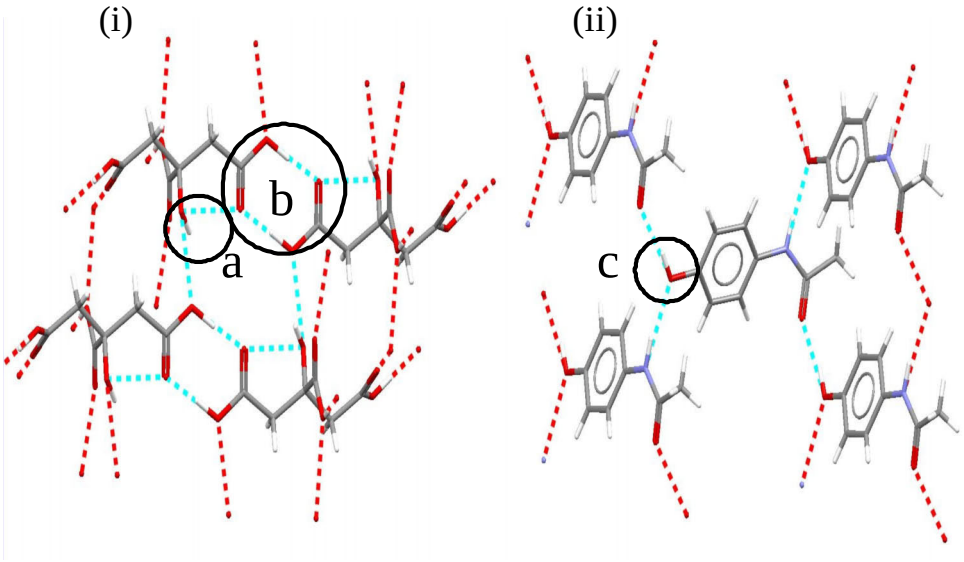

Figure 15 *Molecular interactions in crystalline (i) citric acid anhydrate (CITRAC10) [185] (ii) monoclinic paracetamol (HXACAN07) [183]. Molecular interactions: b, dimerisation of carboxylic acids, a, alcoholic -OH of CAA and c, alcoholic –OH of PARA. Modified from papers I and V.*

There are more opportunities to form hydrogen bonds in CAA than in PARA, which may have an effect on molecular interactions. Therefore, the crystallisation rate of pure CAA is slower than that observed for pure PARA (I). Molecules with multiple hydroxyl groups, such as sugars, are known to produce amorphous form quite easily [85]. The aromatic ring is reported to cause steric hindrance that restricts the hydrogen bond network from growing uniformly in one direction in m-toluidine glass [108]. This could be one explanation for why blends are physically more stable than pure materials in our study. Apparently, a blend should be less ordered than a pure substance, which could have an effect on the crystallisation rate. Thus, molecular interactions such as hydrogen bonds combined with van der Waals forces might have an effect on the crystallisation tendency of amorphous materials (I, V), at least within amorphous blends with a low T_g.

5.2.4 Homogeneity of materials (I, II, V)

For all the materials measured, a single glass transition temperature was observed indicating the good miscibility of the blends. However, DSC is not the most sensitive method to measure miscibility of the blend [202]. Proton rotating-frame spin-lattice relaxation constants ($T_{1\rho}$) were quite similar when probed via different ^{13}C atoms in the amorphous blend, confirming a good homogeneity in the blends. However, the standard deviation in the $T_{1\rho}$ was

found to be smaller for the 50/50 (w/w, %) blend than for other blends, which might be related to the better miscibility of this system compared with other systems. Thus, the crystallisation tendency of blends such as 75/25 (PARA/CAA, w/w) might be related to a lack of homogeneity due to ineffective blending. Similar behaviour in changes of spectral linewidth as a function of measurement temperature in the ssNMR study revealed similar dynamics for citric acid anhydrate and paracetamol in the amorphous 50/50 blend. This result confirmed the good homogeneity of the material, which was a prerequisite for good physical stability of the 50/50 blend.

5.2.5 Other prerequisites for physical stability (I, II, V)

There might also be some other factors that are important for stabilising the amorphous binary mixtures besides molecular interactions and good homogeneity of materials, such as the thermodynamic and crystallisation driving forces (II, V). Especially formation of the "eutectic mixture" (i.e. physical mixture of 50/50 blend has the lowest melting point) of the CAA/PARA blend [109] might be a key factor leading to a decrease in the thermodynamic driving force for crystallisation [203] of the 50/50 blend.

One possible reason for this could be the high viscosity of the 50/50 blend just above the T_g as seen in paper II. In the blends, there is always more than one molecular species, increasing the mismatch between molecular networks. Similarly, the benzene ring of PARA may cause steric hindrance in the blends and stabilise electrostatic forces with other electron donating groups, as suggested by Timko (1979) [109]. Differences in T_g cannot be the reason for the good physical stability of the blends because the blends had lower T_g's than pure PARA, but nonetheless PARA was more stable in the blends than as a pure substance. A similar effect has been reported for a case where glycerol increased the chemical stability of a material, even though the T_g decreased and molecular mobility increased [204]. Similarly, small amount of water in the material, i.e. no plasticising effect, has been suggested to be beneficial in amorphous material because of possible changes in free volume or structure of material [204,205].

5.3 Ultrasound-assisted processing

Thus far, researchers have been interested in drugs having a glass transition higher than ambient temperature, because drug systems having a low T_g are thought to be physically too unstable and difficult to handle and process in an industrial scale. Thus, a new processing method was developed and patented for a sticky/viscous amorphous material.

5.3.1 Extrusion (III)

Figure 16 shows the effect of ultrasound power and material temperature on mass flow through a 3 mm orifice. Mass flow through the nozzle improved when the temperature or the ultrasound power were increased. The effect of ultrasound on mass flow was not related to the warm-up of the nozzle due to instantaneous changes in the mass flow as the ultrasound power was switched on or switched off. The main reasons for better material flow due to ultrasound may be lower viscosity due to changes in the surface properties of the material and a reduction in the surface friction between metal and material. Similar results have been described in polymer and food studies [166,176]. A decrease in friction has been found to increase die durability and to produce a better surface on the processed extrudates in polymer extrusion [176,206]. Air bubbles in the material were problematic during the processing because they started to oscillate when ultrasound power was used, and this breaks down the extrudate. This effect was extremely strong if there was a high amount of bubbles in the material.

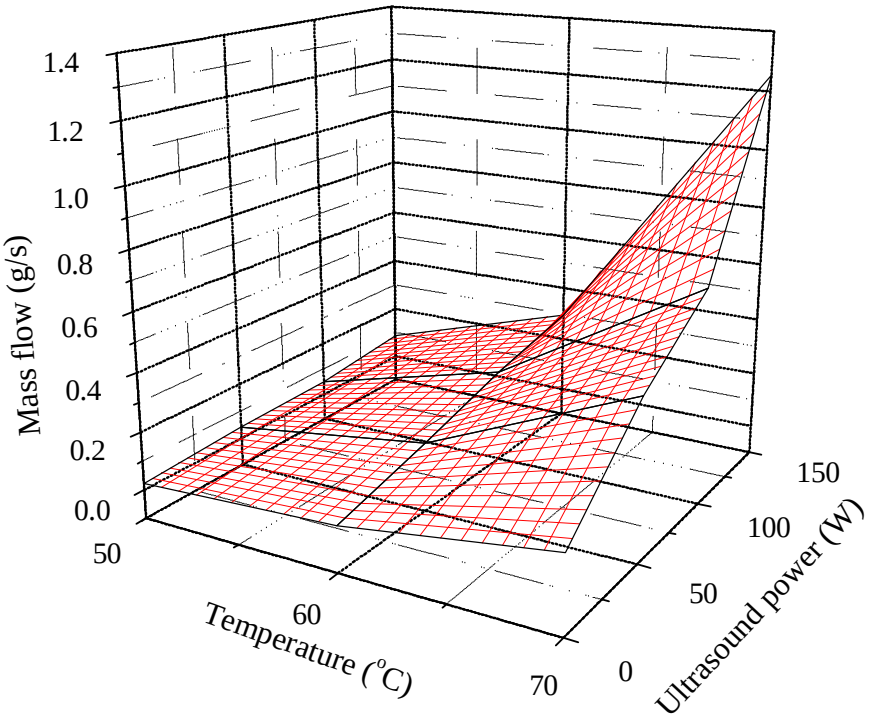

Figure 16 *Effect of ultrasound power (W) on mass flow as a function of temperature (°C) through an ultrasound assisted nozzle. Modified from paper III.*

5.3.2 Cutting (III)

The 50/50 blend was found to be sticky in our probe tack test but it was possible to handle this material with ultrasound. The reasons for stickiness (III) were assumed to be: glass transition, viscosity, time-dependent wetting and surface energetics.

Ultrasound cutting was found to be a good method of cutting amorphous sticky model material compared with traditional cutting where the material stuck to the blade (Table 11). Different ultrasound power levels (50 and 100 W) were not observed to have an effect on the quality and appearance of cut extrudates. The best cutting temperature for this material was found to be approximately 40-50 °C because it gave nice sharp corners for the extrudate cuts.

One reason why ultrasound decreased the stickiness was that the vibrating metal surface decreases the contact time needed to achieve good wetting on the blade. The other possible reason was the bubbles in the cracks on the blade surface. These air bubbles started to cavitate/oscillate when ultrasound was used [162], hindering contact between the knife and sticky material. One possible problem in ultrasound cutting has been the heat generated by the cutting [179]. However, the cutting time would have to be rather long, whereas the cutting process normally only requires milliseconds.

The average weight of the 5 mm long extrudate was approximately 13 mg. These units can be used to fill capsules. Approximately 200 mg of drug could be processed into a single extrudate/dosage form if the diameter of the orifice in the nozzle is increased to 8 mm and length of extrudate would be 10 mm. This size of extrudate could be used to fill capsules or could be further processed by coating.

Table 11. *Effect of ultrasound on sticking of extrudate to the knife (yes / no) [a] and appearance of the edge of the extrudate (broke down during cutting / sharp / round / squashed) [b].*

US* power [W]/ Cutting temp. [°C]	0 W	50 W	100 W
25 °C	[(a)] yes	[(a)] no	[(a)] no
	[(b)] broke down	[(b)] broke down	[(b)] broke down
40 °C	[(a)] yes	[(a)] no	[(a)] no
	[(b)] squashed	[(b)] sharp	[(b)] sharp
50 °C	[(a)] yes	[(a)] no	[(a)] no
	[(b)] squashed	[(b)] sharp	[(b)] sharp
60 °C	[(a)] yes	[(a)] no	[(a)] no
	[(b)] squashed	[(b)] round	[(b)] round

* US, ultrasound

5.3.3 Effect of ultrasound on physical stability of materials (IV)

The ultrasound assisted extrusion and cutting did not accelerate the crystallisation rate of processed materials (IV). A possible reason why these materials did not crystallise during ultrasound treatment was the short contact time with ultrasound and a high viscosity at the processing temperature. Ultrasound treatment has been reported to have an effect only on the surface of viscous liquids and then treatment time should be long (at least 60 s) to trigger crystallisation [207]. Thus sonocrystallisation processes are done in liquids with low viscosity such as water [43] (viscosity = 10^{-3} Pa·s at 20 °C). Furthermore, cavitation is one of the main factors in the sonocrystallisation process [43,177] but in viscous liquid, cavitation might not occur because microbubbles are unlikely to form due to the viscosity.

Ultrasound cutting and extrusion proved to be useful method for processing amorphous materials and amorphous binary mixtures, provided that the material was sufficiently physically stable against mechanical and thermal stress. In addition, ultrasound as a processing aid could be used to increase the processability of sticky solid dispersions.

A patent application for ultrasound-assisted extrusion and cutting for pharmaceutical use has been filed based on the results reported in this study [181].

6. Conclusions

A blend of citric acid anhydrate (CAA) and paracetamol (PARA) (50/50, %, w/w) was observed to be a good amorphous model substance with a low glass transition temperature for the large scale processing studies.

The composition of the blend and material exposure to water were found to be critical factors affecting the physical stability (i.e. crystallisation) of the amorphous materials. Molecular mobility was not observed to be the main factor for stabilisation of CAA/PARA blends because the molecular relaxation time was less than 100 s in ambient conditions. The factors responsible for the good physical stability of the 50/50 blend were good homogeneity and the molecular interactions in the amorphous binary mixture, and these underlying reasons for its physical stability could be effectively evaluated using ssNMR spectroscopy. Other important factors included the thermodynamic driving force i.e. the formation of the "eutectic mixture". The good physical stability of the 50/50 blend was not related to degradation products. Initial consecutive shearing after sample preparation was found to correlate with the actual physical stability of the materials in long-term storage in dry conditions.

Composition and temperature affected stickiness and deformability of the material. Stickiness was especially dependent on the glass transition and viscosity. With the help of ultrasound extrusion and cutting, it was possible to process sticky amorphous material in the supercooled liquid state. In addition, ultrasound treated materials were not found to crystallise more rapidly than untreated materials during one year of storage in dry conditions. Thus, ultrasound extrusion and cutting are extremely promising processing methods for viscous and sticky material.

7. References

[1] Y. Roos, Phase transitions in foods. Academic press, Inc., USA, 1995, p 360.

[2] B. C. Hancock, G. Zografi, Characteristics and significance of the amorphous state in pharmaceutical systems, J. Pharm. Sci. 86 (1997) 1-12.

[3] M. C. Lai, E. M. Topp, Solid-state chemical stability of proteins and peptides, J. Pharm. Sci. 88 (1999) 489-500.

[4] Ö. Almarsson, C. R. Gardner, Novel approaches to issues of developability, Current Drug Discovery 3 (2003) 21-26.

[5] D. Singhal, W. Curatolo, Drug polymorphism and dosage form design: a practical perspective, Adv. Drug Del. Rev. 56 (2004) 335-347.

[6] G. L. Amidon, H. Lennernäs, V. P. Shah, J. R. Crison, A theoretical basis for a biopharmaceutic drug classification: The correlation of in vitro drug product dissolution and in vivo bioavailability, Pharm. Res. 12 (1995) 413-420.

[7] R. K. Verma, S. Garg, Current status of drug delivery technologies and future directions, Pharm. Tech. On-line 25 (2001) 1-14.

[8] S. Richton-Hewett, E. Foster, C. S. Apstein, Medical and economic consequences of a blinded oral anticoagulant brand change at a municipal hospital, Arch. Intern. Med. 148 (1988) 806-808.

[9] K. Inoue, K. Ogawa, J. i. Okada, K. Sugibayashi, Enhancement of skin permeation of ketotifen by supersaturation generated by amorphous form of the drug, J. Control. Release 108 (2005) 306-318.

[10] G. G. Z. Zhang, D. Law, E. A. Schmitt, Y. Qiu, Phase transformation considerations during process development and manufacture of solid oral dosage forms, Adv. Drug Del. Rev. 56 (2004) 371-390.

[11] C. R. Gardner, C. T. Walsh, Ö. Almarsson, Drugs as materials: Valuing physical form in drug discovery, Nat. Rev. Drug Discovery 3 (2004) 926-934.

[12] Pfizer, Pfizer Annual Report 2006, ed., Pfizer Inc., 2007 p 84.

[13] P. R. Rose, J. A. Leonard, Process form forming amorphous atorvastatin calcium, WO 2005/100313 A1 (2004).

[14] A. T. M. Serajuddin, Solid dispersion of poorly water-soluble drugs: early promises, subsequent problems, and recent breakthroughs, J. Pharm. Sci. 88 (1999) 1058-1066.

[15] K. Yamashita, T. Nakate, K. Okimoto, A. Ohike, Y. Tokunaga, R. Ibuki, K. Higaki, T. Kimura, Establishment of new preparation method for solid dispersion formulation of tacrolimus, Int. J. Pharm. 267 (2003) 79-91.

[16] P. M. V. Gilis, V. F. V. De Conde, R. P. G. Vandecruys, Beads having a core coated with antifungal and a polymer WO9405263A1 (1993).

[17] C. A. Bailey, J. C. Ferdinando, Pharmaceutical composition comprising a proteinase inhibitor and a monoglyceride, WO9639742A1 (1996).

[18] A. M. Kaushal, P. Gupta, A. K. Bansal, Amorphous drug delivery systems: Molecular aspects, design, and performance, Crit. Rev. Ther. Drug. Carrier Syst. 21 (2004) 133-193.

[19] B. C. Hancock, Disordered drug delivery: destiny, dynamics and the deborah number, J. Pharm. Pharmacol. 54 (2002) 737-746.

[20] C. L. Stevenson, D. B. Bennett, D. Lechuga-Ballesteros, Pharmaceutical liquid crystals: The relevance of partially ordered systems, J Pharm. Sci. 94 (2005) 1861-1880.

[21] C. J. Roberts, P. G. Debenedetti, Engineering pharmaceutical stability with amorphous solids, AIChE Journal 48 (2002) 1140-1144.

[22] W. L. Chiou, S. Riegelman, Pharmaceutical applications of solid dispersion systems, J. Pharm. Sci. 60 (1971) 1281-1302.

[23] J. L. Ford, The current status of solid dispersions, Pharm. Acta Helv. 61 (1986) 69-88.

[24] H. R. Guzmán, M. Tawa, Z. Zhang, P. Ratanabanangkoon, P. Shaw, C. R. Gardner, H. Chen, J.-P. Moreau, Ö. Almarsson, J. F. Remenar, Combined use of crystalline salt forms and precipitation inhibitors to improve oral absorption of celecoxib from solid oral formulations, J. Pharm. Sci. 96 (2007) 2686-2702.

[25] W. Wang, Lyophilization and development of solid protein pharmaceuticals, Int. J. Pharm. 203 (2000) 1-60.

[26] R. A. Beyerinck, R. J. Ray, D. E. Dobry, D. M. Settell, Method form making homogeneous spray-dried solid amorphous drug dispersions using pressure nozzles., WO03/063821A2 (2003).

[27] R. A. Beyerinck, R. J. Ray, D. E. Dobry, D. M. Settell, K. R. Spence, H. L. M. Deibele, Method for making homogeneous spray-dried solid amorphous drug dispersions utilizing modified spray-drying apparatus, WO0363822A2 (2003).

[28] Z. Yu, K. P. Johnston, R. O. Williams, Spray freezing into liquid versus spray-freeze drying: Influence of atomization on protein aggregation and biological activity, Eur. J. Pharm. Sci. 27 (2006) 9-18.

[29] O. L. Sprockel, M. Sen, P. Shivanand, W. Prapaitrakul, A melt-extrusion process for manufacturing matrix drug delivery systems, Int. J. Pharm. 155 (1997) 191-199.

[30] L. Yu, D. S. Mishra, D. R. Rigsbee, Determination of the glass properties of D-mannitol using sorbitol as an impurity, J. Pharm. Sci. 87 (1998) 774-777.

[31] D. Giron, Characterisation of salts of drug substances, J. Therm. Anal. Cal. 73 (2003) 441-457.

[32] L. Yu, Amorphous pharmaceutical solids: preparation, characterization and stabilization, Adv. Drug Del. Rev. 48 (2001) 27-42.

[33] J. K. Guillory, Generation of polymorphs, hydrates, solvates, and amorphous solids, in: H. G. Brittain, editor Polymorphs in pharmaceutical solids: Marcel Dekker, Inc., NY, USA 1999, pp 183-226.

[34] Y. Li, J. Han, G. G. Z. Zhang, D. J. W. Grant, R. Suryanarayanan, In situ dehydration of carbamazepine dihydrate: A novel technique to prepare amorphous anhydrous carbamazepine, Pharm. Dev. Tech. 5 (2000) 257-266.

[35] J. E. Patterson, B. J. Michael, A. H. Forster, R. W. Lancaster, J. M. Butler, T. Rades, The influence of thermal and mechanical preparative techniques on the amorphous state of poorly soluble compunds, J. Pharm. Sci. 94 (2005) 1998-2012.

[36] T. J. Smith, G. Gauzer, High pressure compaction for pharmaceutical formulations, WO2004058222A1 (2003).

[37] S. Weinhold, M. Litt, J. B. Lando, The effect of crystallite on the electric field induced α to δ crystals phase transition in poly(vinylodene fluoride), Ferroelectrics 57 (1984) 277-296.

[38] S. F. Swallen, K. L. Kearns, M. K. Mapes, Y. S. Kim, R. J. McMahon, M. D. Ediger, T. Wu, L. Yu, S. Satija, Organic glasses with exceptional thermodynamic and kinetic stability, Science 315 (2007) 353-356.

[39] S. Szoke, C. Szabo, L. Gyuricza, C. Singer, V. Niddam-Hildesheim, G. Sterimbaum, Process for preparation of amorphous form of a drug, WO2005/117837A1 (2005).

[40] A. M. Abdul-Fattah, D. Lechuga-Ballesteros, D. S. Kalonia, M. J. Pikal, The impact of drying method and formulation on the physical properties and stability of

methionyl human growth hormone in the amorphous solid state, J. Pharm. Sci. 97 (2008) 163-184.

[41] F. Igantious, L. Sun, Electrospun amorphous pharmaceutical compositions, WO2004014304A2 (2003).

[42] K. S. Suslick, G. J. Price, Applications of ultrasound to materials chemistry, Annu. rev. Mater. Sci. 29 (1999) 295-326.

[43] G. Ruecroft, D. Hipkiss, T. Ly, N. Maxted, P. W. Cains, Sonocrystallization: The use of ultrasound for improved industrial crystallization, Org. Process Res. Dev. 9 (2005) 923-932.

[44] T. Yamaguchi, M. Nishimura, R. Okamoto, T. Takeuchi, K. Yamamoto, Glass formation of 4"-O-(4-methoxyphenyl) acetyltylosin and physicochemical stability of the amorphous solid, Int. J. Pharm. 85 (1992) 87-96.

[45] E. Shalaev, G. Zografi, The concept of "structure" in amorphous solids from the perspective of the paharmaceutical sciences, in: H. Levine, editor Amorphous food and pharmaceutical systems, Cambridge: The Royal Society of Chemistry, 2002, pp 11-30.

[46] L. H. Sperling, Introduction to physical polymer science. John Wiley & Sons Inc. New York., 1992, p 594.

[47] P. W. Anderson, Viewpoint: The future, Science 267 (1995) 1615-1616.

[48] W. Kauzmann, The nature of the glassy state and the behavior of liquids at low temperatures, Chem. Rev. 43 (1948) 219-256.

[49] N. E. Cusack, The physics of structurally disordered matter. An introduction. IOP Publishing Ltd., Bristol, England, 1987, p 402.

[50] C. T. Moynihan, A. J. Easteal, J. Wilder, Dependence of the glass transition temperature on heating and cooling rate, J. Phys. Chem. 78 (1974) 2673-2677.

[51] M. D. Ediger, C. A. Angell, S. R. Nagel, Supercooled liquids and glasses, J. Phys. Chem. 100 (1996) 13200-13212.

[52] K.-L. Li, A. A. Jones, P. T. Inglefield, Domain size of dynamic heterogeneities just above the glass transition in an amorphous polycarbonate, Macromolecules 22 (1989) 4198-4204.

[53] M. D. Ediger, Movies of the glass transition, Science 287 (2000) 604-605.

[54] L. Slade, H. Levine, Beyond water activity: Recent advances based on an alternative approach to the assessment of food quality and safety, Crit. Rev. Food Sci. Nutr. 30 (1991) 115-360.

[55] D. Champion, M. Le Meste, D. Simatos, Towards an improved understanding of glass transition and relaxations in foods: molecular mobility in the glass transition range, Trends Food Sci. Tech. 11 (2000) 41-55.

[56] G. W. White, S. H. Cakebread, The glassy state in certain sugar-containing food products, J. Fd Technol. 1 (1966) 73-82.

[57] Y. Roos, M. Karel, Effect of glass transitions on dynamic phenomena in sugar containing food systems, in: J. M. V. Blanshard, P. J. Lillford, editors, The glassy state in foods: Nottingham University Press, England, 1993, pp 207-222.

[58] Y. H. Roos, S. M. Lievonen, State transitions and reaction rates in concentrated food systems, in: J. Welti-Chanes, G. V. Barbosa-Canovas, J. M. Aguilera, editors, Engineering and food for the 21st century: CRC Press LLC, Boca Raton, 2002, pp 67-86.

[59] J. M. Hutchinson, Physical aging of polymers, Prog. Polym. Sci. 20 (1995) 703-760.

[60] C. Mao, S. P. Chamarthy, R. Pinal, Time-dependence of molecular mobility during structural relaxation and its impact on organic amorphous solids: An investigation based on a calorimetric approach Pharm. Res. 23 (2006) 1906-1917.

[61] M. Le Meste, D. Champion, G. Roudaut, G. Blond, D. Simatos, Glass transition and food technology: A critical appraisal, J. Food Sci. 67 (2002) 2444-2458.

[62] K.-H. Illers Von, Einfluss der thermischen Vorgeschichte auf die Eigenschaften von polyvinylchlorid, Makromol. Chemie 127 (1970) 1-33.

[63] J. C. Arnold, The effects of physical aging on the brittle fracture behavior of polymers, Polym. Eng. Sci. 35 (1995) 165-169.

[64] A. C.-M. Yang, R. C. Wang, J. H. Lin, Ductile-brittle transition induced by aging in poly(phenylene oxide) thin films, Polymer 37 (1996) 5751-5754.

[65] S. Mukherjee, S. A. Jabarin, Aging characteristics of oriented poly(ethylene terephthalate), Polym. Eng. Sci. 35 (1995) 1145-1154.

[66] L. W. Vick, R. G. Kander, Physical aging effects in the compaction and sintering of polycarbonate powder, Plastics- Rasing into the future: Society of plastics engineers, 1996, pp 1960-1964.

[67] V.-T. Truong, B. C. Ennis, Effect of physical aging on the fracture behavior of crosslinked epoxies, Polym. Eng. Sci. 31 (1991) 548-557.

[68] S. Vyazovkin, I. Dranca, Effect of physical aging on nucleation of amorphous indomethacin, J. Phys. Chem. B 111 (2007) 7283-7287.

[69] A. Tanaka, K.-h. Nitta, R. Maekawa, T. Masuda, T. Higashimura, Effects of physical aging on viscoelastic and ultrasonic properties of poly[1-(trimethylsilyl)-1-propyne] films, Polym. J. 24 (1992) 1173-1180.

[70] A. M. Abdul-Fattah, K. M. Dellerman, R. H. Bogner, M. J. Pikal, The effect of annealing on the stability of amorphous solids: Chemical stability of freeze-dried moxalactam, J. Pharm. Sci. 96 (2007) 1237-1250.

[71] M. J. Pikal, R. D. Reddy, E. Y. Shalaev, C. B. Ziegler, Method of stabilizing disordered cefovecin sodium salt, WO2005/102274 A2 (2005).

[72] R. D. Reddy, E. Y. Shalaev, R. M. Shanker, C. B. Ziegler, Process for annealing amorphous atorvastatin, CA2547216A1 (2005).

[73] B. C. Hancock, S. L. Shamblin, G. Zografi, Molecular mobility of amorphous pharmaceutical solids below their glass transition temperatures, Pharm. Res. 12 (1995) 799-806.

[74] C. Bhugra, M. J. Pikal, Role of thermodynamic, molecular, and kinetic factors in crystallization from the amorphous state, J Pharm. Sci. 97 (2008) 1329-1349.

[75] S. R. Ovshinsky, Chemistry and structure in amorphous materials: The shapes of things to come, in: D. Adler, H. Fritzsche, S. R. Ovshinsky, editors, Physics of disordered materials: Plenum Press, New York, USA, 1985, pp 37-54.

[76] S. D. Allison, B. Chang, T. W. Randolph, J. F. Carpenter, Hydrogen bonding between sugar and protein is responsible for inhibition of dehydration-induced protein unfolding, Arch. Biochem. Biophys. 365 (1999) 289-298.

[77] E. Fukuoka, M. Makita, S. Yamamura, Glassy state of pharmaceuticals. III. Thermal properties and stability of glassy pharmaceuticals and their glass systems, Chem. Pharm. Bull. 37 (1989) 1047-1050.

[78] Ö. Almarsson, M. J. Zaworotko, Crystal engineering of the composition of pharmaceutical phases. Do pharmaceutical co-crystals represent a new path to improved medicines?, Chem. Commun. (2004) 1889-1896.

[79] D. L. Price, Intermediate-range order in glasses, Curr. Opin. Solid State Mater. Sci. 1 (1996) 572-577.

[80] S.-J. Kim, T. E. Karis, Glass formation from low molecular weight organic melts, J. Mater. Res. 10 (1995) 2128-2136.

[81] G. Van den Mooter, M. Wuyts, N. Blaton, R. Busson, P. Grobet, P. Augustijns, R. Kinget, Physical stabilisation of amorphous ketoconazole in solid dispersions with polyvinylpyrrolidone K25, Eur. J. Pharm. Sci. 12 (2001) 261-269.

[82] J. L. Keddie, R. A. L. Jones, R. A. Cory, Interface and surface effects on the glass-transition temperature in thin polymer films, Faraday Discuss. 98 (1994) 219-230.

[83] E. Fukuoka, M. Makita, S. Yamamura, Some physicochemical properties of glassy indomethacin, Chem. Pharm. Bull. 34 (1986) 4314-4321.

[84] A. R. Paradkar, B. Chauhan, B. Yamamura, A. P. Pawar, Preparation and characterization of glassy celecoxib, Drug Dev. Ind. Pharm. 29 (2003) 739-744.

[85] G. S. Parks, H. M. Huffman, F. R. Cattoir, Studies on glass. II. The transition between the glassy and liquid states in the case of glucose, J. Phys. Chem. 32 (1928) 1366-1379.

[86] K. C. Fox, Putting proteins under glass, Science 267 (1995) 1922-1923.

[87] Y. Guo, S. R. Byrn, G. Zografi, Physical characteristics and chemical degradation of amorphous quinapril hydrochloride, J. Pharm. Sci. 89 (2000) 128-143.

[88] S. Yoshioka, Y. Aso, Correlations between molecular mobility and chemical stability during storage of amorphous pharmaceuticals, J. Pharm. Sci. 96 (2007) 960-981.

[89] E. Vittadini, P. Chinachoti, J. P. Lavoie, X. Pham, Correlation of microbial response in model food systems with physico-chemical and "mobility" descriptors of the media, Innov. Food Sci. Emerg. 6 (2005) 21-28.

[90] N. Okamoto, M. Oguni, Discovery of crystal nucleation proceedings much below the glass transition temperature in a supercooled liquid, Solid State Commun. 99 (1996) 53-56.

[91] Y. Roos, M. Karel, Crystallization of amorphous lactose, J. Food Sci. 57 (1992) 775-777.

[92] I. Alig, D. Braun, R. Landgendorf, M. Voigt, J. H. Wendorff, Simultaneous ageing and crystallization processes within the glassy state of a low molecular weight substance, J. Non-Cryst. Sol. 221 (1997) 261-264.

[93] C. Mao, S. P. Chamarthy, S. R. Byrn, R. Pinal, A calorimetric method to estimate molecular mobility of amorphous solids at relatively low temperatures, Pharm. Res. 23 (2006) 2269-2276.

[94] G. Adam, J. H. Gibbs, On the temperature dependence of cooperative relaxation properties in glass-forming liquids, J. Chem. Phys. 43 (1965) 139-146.

[95] I. M. Hodge, Effects of annealing and prior history on enthalpy relaxation in glassy polymers. 6. Adam-Gibbs formulation of nonlinearity, Macromolecules 20 (1987) 2897-2908.

[96] R. Böhmer, K. L. Ngai, C. A. Angell, D. J. Plazek, Nonexponential relaxations in strong and fragile glass formers, J. Chem. Phys. 99 (1993) 4201-4209.

[97] K. J. Crowley, G. Zografi, The use of thermal methods for predicting glass-former fragility, Thermochim. Acta 380 (2001) 79-93.

[98] Q. Lu, G. Zografi, Properties of citric acid at the glass transition, J. Pharm. Sci. 86 (1997) 1374-1378.

[99] D. Q. M. Craig, P. G. Royall, V. L. Kett, M. L. Hopton, The relevance of the amorphous state to pharmaceutical dosage forms: glassy drugs and freeze dried systems, Int. J. Pharm. 179 (1999) 179-207.

[100] S. L. Shamblin, E. Y. Huang, G. Zografi, The effects of co-lyophilized polymeric additives on the glass transition temperature and crystallization of amorphous sucrose, J. Therm. Anal. 47 (1996) 1567-1579.

[101] S. L. Shamblin, L. S. Taylor, G. Zografi, Mixing behavior of colyophilized binary systems, J. Pharm. Sci. 87 (1998) 694-701.

[102] L. Yu, S. M. Reutzel-Edens, C. A. Mitchell, Crystallization and polymorphism of conformationally flexible molecules: Problems, patterns, and strategies, Org. Process Res. Dev. 4 (2000) 396-402.

[103] J. F. Carpenter, S. C. Hand, L. M. Crowe, J. H. Crowe, Cryoprotection of phosphofructokinase with organic solutes: Characterization of enhanced protection in the presence of divalent cations, Arch. Biochem. Biophys. 250 (1986) 505-512.

[104] B. S. Chang, B. S. Kendrick, J. F. Carpenter, Surface-induced denaturation of proteins during freezing and its inhibition by surfactants, J Pharm. Sci. 85 (1996) 1325-1330.

[105] P. Rongère, N. Morel-Desrosiers, J.-P. Morel, Interactions between cations and sugars. Part 8.—Gibbs energies, enthalpies and entropies of association of divalent and trivalent metal cations with xylitol and glucitol in water at 298.15 K, J. Chem. Soc., Faraday Trans. 91 (1995) 2771 - 2777.

[106] Y. You, R. D. Ludescher, The effect of sodium chloride on molecular mobility in amorphous sucrose detected by phosphorescence from the triplet probe erythrosin B, Carbohydr. Res. 343 (2008) 350-363.

[107] R. B. Singh, P. M. Kumar, R. Malik, Formulations of atorvastatin stabilized with alkali metal additions, EP1336405A1 (2003).

[108] D. Morineau, C. Alba-Simionesco, Hydrogen-bond-induced clustering in the fragile glass-forming liquid m-toluidine: Experiments and simulations, J. Chem. Phys. 109 (1998) 8494-8503.

[109] R. J. Timko, Thermal characterization of glass dispersion systems, ed., Rutgers, The state university of New Jersey-New Brunswick, Rutgers, The State University of New Jersey-New Brunswick, 1979 p 197.

[110] H. Kageyama, K. Itano, W. Ishikawa, Y. Shirota, Striking effects of halogen substituents on the glass properties, glass transition temperatures and stabilities of the glassy state of a new family of amorphous molecular materials, 1,3,5- tris (4-halogenophenylphenyloamino)benzenes, J. Mater. Chem. 6 (1996) 675-676.

[111] P. Tong, L. S. Taylor, G. Zografi, Influence of alkali metal counterions on the glass transition temperature of amorphous indomethacin salts, Pharm. Res. 19 (2002) 649-654.

[112] E. Y. Shalaev, Q. Lu, M. Shalaeva, G. Zografi, Acid-catalyzed inversion of sucrose in the amorphous state at very low levels of residual water, Pharm. Res. 17 (2000) 366-370.

[113] Y. Song, R. L. Schowen, R. T. Borchardt, E. M. Topp, Effect of pH on the rate of asparagine deamidation in polymeric formulations: pH-rate profile, J. Pharm. Sci. 90 (2001) 141-156.

[114] Y. Chikaraishi, M. Otsuka, Y. Matsuda, Preparation of amorphous and polymorph piretanide and their physicochemical properties and solubilities, Chem. Pharm. Bull. 44 (1996) 1614-1617.

[115] G. Chawla, A. K. Bansal, A comparative assessment of solubility advantage from glassy and crystalline forms of a water-insoluble drug, Eur. J. Pharm. Sci. 32 (2007) 45-57.

[116] H. Konno, L. S. Taylor, Influence of different polymers on the crystallization tendency of molecularly dispersed amorphous felodipine, J. Pharm. Sci. 95 (2006) 2692-2705.

[117] P. Marsac, H. Konno, L. S. Taylor, A comparison of the physical stability of amorphous felodipine and nifedipine systems, Pharm. Res. 23 (2006) 2306-2316.

[118] D. Zhou, G. G. Z. Zhang, D. Law, D. J. W. Grant, E. A. Schmitt, Physical stability of amorphous pharmaceuticals: Importance of configurational thermodynamic quantities and molecular mobility, J. Pharm. Sci. 91 (2002) 1863-1872.

[119] D. Law, S. L. Krill, E. A. Schmitt, J. J. Fort, Y. Qiu, W. Wang, W. R. Porter, Physicochemical considerations in the preparation of amorphous ritonavir-poly(ethylene glycol) 8000 solid dispersion, J. Pharm. Sci. 90 (2001) 1015-1025.

[120] K. Six, G. Verreck, J. Peeters, P. Augustijns, R. Kinget, G. Van den Mooter, Characterization of glassy itraconazole: a comparative study of its molecular mobility below Tg with that of structural analogues using MTDSC, Int. J. Pharm. 213 (2001) 163-173.

[121] T. Miyazaki, S. Yoshioka, Y. Aso, T. Kawanishi, Crystallization rate of amorphous nifedipine analogues unrelated to the glass transition temperature, Int. J. Pharm. 336 (2007) 191-195.

[122] D. Kilcast, C. Roberts, Perception and measurements of stickiness, J. Texture Stud. 29 (1998) 81-100.

[123] B. Adhikari, T. Howes, B. R. Bhandari, V. Truong, Stickiness in foods: A review of mechanism and test methods, Int. J. Food Prop. 4 (2001) 1-33.

[124] E. M. Petrie, Handbook of adhesives and sealants. McGraw-Hill, New York, USA, 2000, p 914.

[125] H. Schubert, Food particle technology. Part I: Properties of particles and particulate food systems, J. Food Eng. 6 (1987) 1-32.

[126] H. Rumpf, Grundlagen und methoden des granulierens, Chem. Eng. Tech. 30 (1958) 144-158.

[127] R. Kunzig, The physics of... tape Why does it stick?, Discover July (1999) 27-29.

[128] C. Gay, L. Leibler, Theory of tackiness, Phys. Rev. Let. 82 (1999) 936-939.

[129] B. Bhandari, T. Howes, Proceedings of International Conference on Innovations in Food Processing Technology and Engineering, Bangkok, Thailand, 2002.

[130] J. M. Aguilera, J. M. del Valle, M. Karel, Caking phenomena in amorphous food powders, Trends Food Sci. Technol. 6 (1995) 149-155.

[131] B. R. Bhandari, T. Howes, Implication of glass transition for the drying and stability of dried foods, J. Food Eng. 40 (1999) 71-79.

[132] G. E. Dowton, J. L. Flores-Luna, J. King, Mechanism of stickiness in hygroscopic, amorphous powders, Ind. Eng. Chem. Fundam. 21 (1982) 447-451.

[133] P. R. Rennie, X. D. Chen, C. Hargreaves, A. R. Meckereth, A study of the cohesion of dairy powders, J. Food. Eng. 39 (1999) 277-284.

[134] Y. Roos, M. Karel, Plasticizing effect of water on thermal behavior and crystallization of amorphous food models, J. Food Sci. 56 (1991) 38-43.

[135] C. Hennings, T. K. Kockel, T. A. G. Langrich, New measurements of the sticky behavior of skim milk powder, Drying Technol. 19 (2001) 471-484.

[136] K. R. Morris, U. J. Griesser, C. J. Eckhardt, J. G. Stowell, Theoretical approaches to physical transformations of active pharmaceutical ingredients during manufacturing processes, Adv. Drug Del. Rev. 48 (2001) 91-114.

[137] S. E. Walker, J. A. Ganley, K. Bedford, T. Eaves, The filling of molten thixotropic formulations into hard gelatin capsules, J. Pharm. Pharmacol. 6 (1980) 389-393.

[138] R. Ritter, Keep cool with cryogenic grinding, Chem. Eng. 104 (1997) 88-93.

[139] M. Wilczek, J. Bertling, D. Hintemann, Optimised technologies for cryogenic grinding, Int. J. Miner. Process. 74S (2004) 425-434.

[140] M. Peleg, M. Hollenbach, Flow conditioners and anticaking agents, Food Technology 38 (1984) 93-102.

[141] G. Buckton, P. Darcy, The influence of additives on the recrystallisation of amorphous spray dried lactose, Int. J. Pharm. 121 (1995) 81-87.

[142] B. C. Hancock, S. L. Shamblin, Water vapour sorption by pharmaceutical sugars, Pharm. Sci. Technol. To. 1 (1998) 345-351.

[143] M. J. Pikal, K. M. Dellerman, M. L. Roy, R. M. Riggin, The effects of formulation variables on the stability of freeze -dried human growth hormone, Pharm. Res. 8 (1991) 427-436.

[144] S. Tsourouflis, J. M. Flink, M. Karel, Loss of structure in freeze-dried carbohydrates solutions: Effect of tmperature, moisture content and composition, J. Sci. Fd Agric. 27 (1976) 509-519.

[145] B. R. Bhandari, N. Datta, R. Crooks, T. Howes, S. Rigby, A semi-empirical approach to optimise the quantity of drying aids required to spray dry sugar-rich foods, Drying Technol. 15 (1997) 2509-2525.

[146] D. Q. M. Craig, The mechanisms of drug release from solid dispersions in water-soluble polymers, Int. J. Pharm. 231 (2002) 131-144.

[147] C. Karlsson, P. J. Lundberg, A. Rosinski, M. Soderbom, Polyethylene glycol matrix pellets for greasy, oily or sticky drug substances, US 6,555,138 B1. (2004).

[148] P. Chiesi, L. Pavesi, pharmaceutical compositions containing ipriflavone, rrocess for the preparation thereof and relative therapeutic use, EP0521057B1 (1991).

[149] S. Yanai, K. Sudo, Y. Akiyama, N. Nagahara, Oral composition of fumagillol derivative, US5846562 (1997).

[150] A. J. Humberstone, W. N. Charman, Lipid-based vehicles for the oral delivery of poorly water soluble drugs, Adv. Drug Del. Rev. 25 (1997) 103-128.

[151] J. Breitenbach, J. Rieger, J. Rosenberg, Long-Shelf-life medicaments, WO 96/29060 (1995).

[152] J. Rosenberg, G. Berndl, B. Liepold, J. Breitenbach, Mechanically stable pharmaceutical presentations form containing liquid or semisolid surface-active substances, US 6599528B1 (2000).

[153] S. Host, J. Tsai, Use of oil adsorbent natural polymer for cosmetic and pharmaceutical applications, EP0659403A2 (1994).

[154] B. Breton, T. Mikolajczyk, F. Ollevier, I. Roelants, Oral delivery form having a high absorption efficiency and methods for making same, WO97/40702 (1996).

[155] E. Perrier, C. Buffevant, Polysaccharide wall microcapsules containing primary alcohol functions and compositions containing same, US005562924A (1993).

[156] K. Kumabe, H. Yanaka, T. Kondo, J. Shirai, Stabilizing agent for aleaginous, physiologically active substances, US005853761A (1996).

[157] K. Kumabe, Core substance-containing calcium microparticles and methods for producing the same, US00615904A (1999).

[158] A. Shoh, Industrial applications of ultrasound- A review. I. High-power ultrasound, IEEE Trans. Sonics and Ultrasonics 22 (1975) 60-71.

[159] N. Denbow, Ultrasonic instrumentation in the food industry, in: E. Kress-Rogers, C. J. B. Brimelow, editors, Instrumentation and Sensors for the Food Industry (2nd Edition): Woodhead Publishing and CRC Press LCC, USA., 2001, pp 326-354.

[160] J. D. McClements, Advances in the application of ultrasound in food analysis and processing, Trends. Food Sci. Technol. 6 (1995) 293-299.

[161] T. J. Mason, Sonochemistry. New York, Oxford University Press, 1999, p 92.

[162] J. R. Frederick, Ultrasonic engineering. John Wiley & Sons,Inc., USA., 1965, p 382.

[163] M. Levina, M. H. Rubinstein, The effect of ultrasonic vibration on the compaction caharacteristics of paracetamol, J. Pharm. Sci. 89 (2000) 705-723.

[164] N. Passerini, B. Albertini, B. Perissutti, L. Rodriguez, Evaluation of melt granulation and ultrasonic spray congealing as techniques to enhance the dissolution of praziquantel, Int. J. Pharm. 318 (2006) 92-102.

[165] A. Mulet, J. Cárcel, J. Benedito, C. Rosselló, S. Simal, Ultrasonic mass transfer enhancement in food processing, in: J. Welti-Chanes, J. F. Vélez-Ruiz, G. V. Barbosa-Cánovas, editors, Transport phenomena in food processing: CRC press LLC , USA., 2003, pp chp. 18.

[166] D. Knorr, M. Zenker, V. Heinz, L. Dong-Un, Applications and potential of ultrasonics in food processing, Trends. Food Sci. Technol. 15 (2004) 261-266.

[167] S.-J. Liu, Y.-E. Tsai, S. Wen-Neng Ueng, E.-C. Chan, A novel solvent-free method for the manufacture of biodegradable antibiotic-capsules for a long-term drug release using compression sintering and ultrasonic welding techniques, Biomaterials 26 (2005) 4662-4669.

[168] M. Midler Jr., Production of crystals in a fluidized bed with ultrasonic vibrations, US3510266 (1970).

[169] V. S. Moholkar, M. M. C. G. Warmoeskerken, Investigation in mass transfer enhancement in textiles with ultrasound, Chem. Eng. Sci. 59 (2004) 299-311.

[170] H. Kim, J. G. Ryu, H. Yang, J. W. Lee, Compatiblization of PC-San blends by ultrasound-assisted mixing, Antec (2003) 2333-2337.

[171] W. Beckham, J. Good, J. Zhan, Dilation of polymeric amorphous regions, ed., National textile center annual report, 1996 p 146-147.

[172] J. Stor-Pellinen, E. Hæggström, M. Luukkala, Measurement of the effect of high-power ultrasound on wetting of paper, Ultrasonics 38 (2000) 953-959.

[173] M. Breitbach, D. Bathen, Influence of ultrasound on adsorption processes, Ultrason. Sonochem. 8 (2001) 277-283.

[174] J. D. Floros, H. Liang, Acoustically assisted diffusion through membranes and biomaterials, Food Technol. 48 (1994) 79-84.

[175] T. Iwasaki, B. Lindberg, H. Meier, The effect of ultrasonic treatment on individual food fibres, Svensk Papperstidning 20 (1962) 795-816.

[176] S. Guo, Y. Li, G. Chen, H. Li, Ultrasonic improvement of rheological and processing behaviour of LLDPE during extrusion, Polym. Int. 52 (2003) 68-73.

[177] T. J. Mason, Power ultrasound in food processing, in: M. J. W. Povey, T. J. Mason, editors, Ultrasound in food processing: Blackie Academic & Professional, Great Brittain, 1998, pp 105-126.

[178] F. F. Rawson, An introduction to ultrasonic food cutting, in: M. J. W. Povey, T. J. Mason, editors, Ultrasound in food processing: Blackie Academic & Professional, Great Brittain, 1998, pp 254-269.

[179] T. A. Emam, A. Cuschieri, How safe is high-power ultrasonic dissection?, Ann. Surg. 237 (2003) 186-191.

[180] Y. Schneider, S. Zahn, J. Hofmann, M. Wecks, H. Rohm, Acoustic cavitation induced by ultrasonic cutting devices: A preliminary study, Ultrason. Sonochem. 13 (2006) 117-120.

[181] P. Hoppu, New pharmaceutical cutting method, Patent Application No. 60/979895, USA (2007).

[182] R. J. Barnes, M. S. Dhanoa, S. J. Lister, Standard normal variate transformation and de-trending of near-infrared diffuse reflectance spectra, Appl. Spectrosc. 43 (1989) 772-777.

[183] G. Nichols, C. S. Frampton, Physicochemical characterization of the orthrorombic polymorph of paracetamol crystallized from solution, J. Pharm. Sci. 87 (1998) 684-693.

[184] G. Roelofsen, J. A. Kanters, Citric acid monohydrate, Cryst. Struct. Comm. 1 (1972) 23-26.

[185] J. P. Glusker, J. A. Minkin, A. L. Patterson, X-ray crystal analysis of the substrates of aconitase. IX. A refinement of the structure of anhydrous citric acid, Acta Cryst. B 25 (1969) 1066-1072.

[186] R. L. Shriner, S. G. Ford, L. J. Roll, Itaconic anhydride and itaconic acid, Org. Synth. 11 (1931) 70.

[187] R. L. Shriner, S. G. Ford, L. J. Roll, Citraconic anhydride and citraconic acid, Org. Synth. 11 (1931) 28.

[188] M. P. Summers, R. P. Enever, Glass transition temperature of citric acid, J. Pharm. Sci. 69 (1980) 612-613.

[189] V. Truong, B. R. Bhandari, T. Howes, B. Adhikari, Analytical model for the prediction of glass transition temperature of food systems, in: H. Levine, editor Amorphous food and pharmaceutical systems, Cambridge: The Royal Society of Chemistry, 2002, pp 31-47.

[190] A. Beuford, Amorphous drug beads, US7163700 B2 (2002).

[191] L. N. Bell, T. P. Labuza, Moisture sorption. Practical aspects of isotherm measurement and use. The American Association of Cereal Chemists Inc., USA., 2000, p 122.

[192] V. Andronis, M. Yoshioka, G. Zografi, Effects of sorbed water on the crystallization of indomethacin from the amorphous state, J. Pharm. Sci. 86 (1997) 346-351.

[193] A. Salameh, L. S. Taylor, Role of deliquescence lowering in enhancing chemical recativity in physical mixtures J. Phys. Chem. B 110 (2006) 10190-10196.

[194] T. E. Karis, S. J. Kim, P. L. Gendler, Y. Y. Cheng, Organic monomeric glass formation by substituted ethylenediamine, J. Non-Cryst. Sol. 191 (1995) 293-303.

[195] J. Petravic, J. Delhommele, Hydrogen bonding in ethanol under shear, J. Chem. Phys. 122 (2005) 1-5.

[196] P. Sherman, Industrial rheology with particular reference to foods, pharmaceuticals and cosmetics. Academic Press, London, UK, 1970, p 423.

[197] R. Pal, Y. Yan, J. H. Masliyah, Rheology of emulsions, in: L. L. Schramm, editor Emulsions: Fundamentals and applications in the petroleum industry, Washington: American Chemical Society, Washington DC, USA, 1992, pp 131-170.

[198] R. J. Hunter, Foundations of colloid science Oxford University Press, Oxford, UK, 1986, p.

[199] G. P. Johari, S. Kim, R. M. Shanker, Dielectric studies of molecular motions in amorphous solid and ultraviscous acetaminophen, J. Pharm. Sci. 94 (2005) 2207-2223.

[200] V. Andronis, G. Zografi, The molecular mobility of supercooled amorphous indomethacin as a function of temperature and relative humidity, Pharm. Res. 15 (1998) 835-842.

[201] C. A. Angell, D. Bressel, R. Green, J. L. Kenno, M. Oguni, E. J. Sare, Liquid fragility and the glass transition in water and aqueous solutions, J. Food Eng. 22 (1994) 115-142.

[202] Y. Aso, S. Yoshioka, T. Miyazaki, T. Kawanishi, K. Tanaka, S. Kitamura, A. Takakura, T. Hayashi, N. Muranush, Miscibility of nifedipine and hydrophilic polymers as measured by ^{1}H-NMR spin–lattice relaxation, Chem. Pharm. Bull. 55 (2007) 1227-1231.

[203] P. I. Buler, Thermodynamic criteria of crystallization from supercooled liquid, Ceram. Int. 16 (1990) 165-169.

[204] M. T. Cicerone, A. Tellington, L. Trost, A. Sokolov, Substantially improved stability of biological agents in dried form, BioProcess International 1 (2003) 36-47.

[205] T. R. Noel, R. Parker, S. G. Ring, A comparative study of the dielectric relaxation behaviour of glucose, maltose, and their mixtures with water in the liquid and glassy states, Carb. Res. 282 (1996) 193-206.

[206] J. Casulli, J. R. Clermont, The oscillating die: A useful concept in polymer extrusion, Polym. Eng. Sci. 30 (1990) 1551-1556.

[207] A. Van Hook, F. Frulla, Nucleation in sucrose solutions, Ind. Eng. Chem. 44 (1952) 1305-1308.